The sensitivity of photosynthesis to O_2 and CO_2 concentration identifies strong Rubisco control above the thermal optimum

Sensitivity of photosynthesis to gas composition identifies photosynthetic limitations

Florian A. Busch[1,2] and Rowan F. Sage[2]

[1]Research School of Biology, The Australian National University, Acton ACT 2601, Australia

[2]Department of Ecology and Evolutionary Biology, The University of Toronto, Toronto, ON, Canada, M5S 3B2

Corresponding author:
Florian Busch
Plant Science Division
Research School of Biology
46 Sullivans Creek Road
The Australian National University
Acton, ACT, 2601
Australia

Tel: +61 2 6125 0123
Email: florian.busch@anu.edu.au

Total word count (excl. summary, references and legends): 6833
Summary: 196
Introduction: 1278
Theoretical Background: 1091
Materials and Methods: 927
Results: 1760
Discussion: 1750
Acknowledgements: 27

No. of Tables: 1
No. of Figures: 9 (Figs. 2-9 in color)
No. of Supporting Information files: 1 (Figs. S1-S5; Notes S1-S2)

Summary

1. The biochemical model of C_3 photosynthesis by Farquhar, von Caemmerer and Berry (FvCB) assumes that photosynthetic CO_2 assimilation is limited by one of three biochemical processes that are not always easily discerned. This leads to improper assessments of biochemical limitations that limit the accuracy of the model predictions.
2. We use the sensitivity of rates of CO_2 assimilation and photosynthetic electron transport to changes in O_2 and CO_2 concentration in the chloroplast to evaluate photosynthetic limitations.
3. Assessing the sensitivities to O_2 and CO_2 concentrations reduces the impact of uncertainties in the fixed parameters to a minimum and simultaneously entirely eliminates the need to determine the variable parameters of the model, such as V_{cmax}, J, or T_P. Our analyses demonstrate that Rubisco limits carbon assimilation at high temperatures, while it is limited by triose phosphate utilization at lower temperatures and at higher CO_2 concentrations.
4. Measurements can be assigned *a priory* to one of the three functions of the FvCB model, allowing testing for the suitability of the selected fixed parameters of the model. This approach can improve the reliability of photosynthesis models on scales from the leaf level to estimating the global carbon budget.

Keywords: photosynthesis, O_2 sensitivity, Rubisco, gas exchange, chlorophyll fluorescence, biochemical model, triose phosphate utilization

Introduction

Theoretical models of carbon assimilation are important tools for interpreting biochemical processes controlling photosynthesis in leaves. In particular, the model of Farquhar, von Caemmerer and Berry (1980) and its derivatives, or FvCB models, are now widely utilized for a range of applications, from predicting the rate of photosynthetic CO_2 exchange (A; acronyms are listed in Table 1) at the leaf level to large scale models of the global carbon cycle and vegetation feedbacks on climate (Farquhar *et al.*, 2001). FvCB models are also commonly used to predict scenarios that are difficult to measure, such as large-scale fluxes or photosynthesis and the carbon cycling in future climate scenarios (Sellers *et al.*, 1997; Prentice *et al.*, 2007). Modeled outputs, however, depend on input parameters, which are often assumed rather than directly determined for plants under study. This leads to the criticism that models can predict a wide range of outcomes, depending upon the input parameters selected, and that researcher's bias can lead to selective use, or "cherry-picking", of enzyme kinetics and other input parameters that enable models to fit experimental data (Ethier & Livingston, 2004).

Critical input parameters for the FvCB model are the kinetic constants of Rubisco, Rubisco activation state, photosynthetic electron transport rate, triose phosphate utilization (TPU) capacity, mesophyll conductance (g_m) and day respiration (R_d). In certain species, such as tobacco and Arabidopsis, most of these values have been empirically measured and thus inputs are relatively well known, particularly at 25°C (von Caemmerer & Quick, 2000; Bernacchi *et al.*, 2001; Bernacchi *et al.*, 2002; Evans & von Caemmerer, 2013; Walker *et al.*, 2013). For all other species, especially at temperatures other than at 25°C, input values are uncertain, leading to guesswork in model parameterization. Modeling efforts have often assumed that the species of choice have the same Rubisco kinetic properties, electron transport properties, and g_m values as tobacco or spinach. Indeed, tobacco and spinach values have been used to model photosynthetic responses in species as diverse as ferns, gymnosperms and a variety of C_3, C_3-C_4, and C_4 angiosperms (see e.g. Medlyn *et al.*, 2002; Massad *et al.*, 2007; Flexas *et*

al., 2014; Gandin *et al.*, 2014). Given the variation between species in Rubisco kinetic properties, electron transport and g_m, the reliance on a select few species for inputs is problematic, particularly when models address thermal responses, evaluate adaptive variation between species or underpin large-scale models of vegetation performance (Friedlingstein *et al.*, 2006; Sage *et al.*, 2008; Booth *et al.*, 2012). As a consequence, important information can be lost or misinterpreted, and conclusions drawn from the model may be dubious.

Only a few studies have measured important modeling parameters such as Rubisco kinetic properties across a wide temperature range (Fig 1a,b; Hermida-Carrera *et al.*, 2016), and these often use different methodologies, which increases variation in the estimates (von Caemmerer & Quick, 2000). These approaches include *in vitro* assays or *in vivo* gas exchange measurements of species with selectively reduced levels of Rubisco, using antisense technology (von Caemmerer *et al.*, 1994). Some of these approaches assume infinite diffusion conductances of CO_2 from the intercellular space to the chloroplast (g_m), while others account for variation in g_m. Recent large species comparisons of Rubisco kinetic properties revealed significant differences even between closely related species (Orr *et al.*, 2016), highlighting that these differences are not only an artifact of differences in measurement protocols. Modeled Rubisco-limited CO_2 assimilation rates strongly depend on the Rubisco kinetic constants used, especially at high temperatures (Galmés *et al.*, 2016). The differences in these constants also contribute to a high variability in the temperature response of the maximum rate of Rubisco carboxylation (V_{cmax}) and photosynthetic electron transport (J_{max}) (Fig. 1c,d; also see e.g. Medlyn *et al.*, 2002). Values of V_{cmax} and J_{max} further depend on various factors such as growth temperature (Yamori *et al.*, 2005; Kattge & Knorr, 2007) and correct estimates of g_m (Ethier & Livingston, 2004; Manter & Kerrigan, 2004), a parameter that also greatly varies with species (von Caemmerer & Evans, 2014). The TPU limitation is often ignored altogether, and temperature responses of TPU are infrequently considered (Harley *et al.*, 1992). As a result of these issues, for effective photosynthetic modeling one is confronted with either direct determination of all the necessary

parameters, or selectively using published parameters that produce reasonable results. Direct determination of the parameters is not feasible for all but a few species due to cost, technical limitations, and substances such as defense compounds that may render biochemical assays impossible. Reliance on published values is also problematic given variation between species and growth conditions in the many model parameters – unless, however, there is an independent means to evaluate the effectiveness of the selected parameters.

Non-invasive techniques that can evaluate the robustness of model inputs are therefore desired. Some have already proven to have good utility, such as online carbon isotope discrimination and pulse-amplitude modulated chlorophyll fluorescence (Pons *et al.*, 2009; Evans & von Caemmerer, 2013). Another possible technique that has not been widely exploited is the sensitivity of A to a variation in O_2 or CO_2 concentration (Sharkey, 1985; Sage & Sharkey, 1987; Sage *et al.*, 1988; Sage *et al.*, 1990; Yamori *et al.*, 2010). O_2 and CO_2 sensitivity measurements can evaluate potential limitations due to Rubisco capacity and electron transport rate, because the sensitivity response depends on the sub-process limiting photosynthesis (Sage & Sharkey, 1987). They can also identify potential TPU limitations (Sharkey, 1985; Sage *et al.*, 1988; Sage *et al.*, 1990). In addition to carbon assimilation, the effect of variation in O_2 and CO_2 concentrations on chlorophyll fluorescence can show responses that are characteristic of the underlying limitation. Thus, the O_2 and CO_2 sensitivity of parameters such as electron transport rate through PSII (*ETR*) and PSII excitation pressure (1-qP) can be used to assess photosynthetic limitations (Sharkey *et al.*, 1988; Ensminger *et al.*, 2006). Compared to using the FvCB model to estimate absolute net CO_2 assimilation rates, an assessment of the O_2 and CO_2 sensitivities can yield robust, independent insights into biochemical limitations of photosynthesis. This is because O_2 and CO_2 sensitivities of A are independent of the variable parameters in the model, such as the maximum rates of carboxylation (V_{cmax}), photosynthetic electron transport (J), or triose phosphate utilization (T_P), which vary between individual leaves. In addition, the parameterization of these sensitivities as a ratio minimizes the impact of uncertainties in the 'fixed'

parameters not estimated by fitting the model, such as Rubisco kinetic constants, since they appear in both the numerator and the denominator.

Rarely have both the O_2 and CO_2 sensitivity of fluorescence and whole-leaf gas exchange been coupled to provide a comprehensive assessment of photosynthetic limitation in C_3 plants (see Sharkey *et al.*, 1988, for an example; however, this study appeared before the modern synthesis of fluorescence analysis improved this approach). Given the wide availability of PAM fluorometers and leaf-level gas exchange machines, it is now possible to examine in depth O_2 and CO_2 sensitivity of both gas exchange and chlorophyll fluorescence to provide a comprehensive evaluation of modeled assumptions. Here, we use sweet potato (*Ipomoea batatas* (L.) Lam.) to demonstrate how O_2 and CO_2 sensitivity can be exploited to test model parameterizations for the CO_2 and temperature response of photosynthesis. We show that this approach allows for *a priori* determinations of the biochemical processes limiting *A* at any given set of conditions. This information can then be used to evaluate the suitability of a set of chosen input parameters. In particular, we use our approach to assess the temperature response of photosynthesis in sweet potato, which was examined and modeled by Cen and Sage (2005), and define biochemical limitations largely independent of the choice of input parameters.

Theoretical Background

The net CO_2 assimilation rate (*A*) at leaf-level has been mechanistically described by the FvCB model as a function of the two competing reactions catalyzed by Rubisco, the carboxylation and oxygenation of ribulose 1,5-bisphosphate (RuBP) (Farquhar *et al.*, 1980; von Caemmerer & Farquhar, 1981; von Caemmerer, 2000), as follows:

$$A = V_c - 0.5V_o - R_d \quad (1)$$

where V_c and V_o denote the rate of RuBP carboxylation and oxygenation, respectively, and R_d stands for the rate of mitochondrial respiration in the light. The net rate of CO_2 uptake is largely determined by the ratio of Rubisco carboxylation to oxygenation, which

depends on the CO_2 concentration in the chloroplast (C_c) and is influenced by leaf temperature. The relation between Rubisco carboxylation and oxygenation is encompassed in Γ^*, the CO_2 compensation point at the site of Rubisco in the absence of mitochondrial respiration, at which photosynthetic CO_2 uptake is equal to photorespiratory CO_2 release. If RuBP supply is not limiting the carboxylation rate of Rubisco, *A* can be described using the RuBP-saturated carboxylation rate, which has a Michaelis-Menten form:

$$A_c = \frac{\left(C_c - \Gamma^*\right) V_{c\max}}{C_c + K_c\left(1 + O / K_o\right)} - R_d \qquad (2)$$

where C_c and O are the CO_2 and O_2 concentrations in the chloroplast and K_c and K_o are the Michaelis-Menten constants of Rubisco for CO_2 and O_2, respectively. The RuBP-saturated carboxylation rate has often been termed the Rubisco-limited assimilation rate, or the RuBP-consumption-limited rate, as it is largely dependent on the maximum rate of carboxylation of Rubisco, V_{cmax} (von Caemmerer, 2000). At elevated CO_2 concentrations (typically above the current ambient of 400 μmol mol^{-1}), the regeneration rate of RuBP lags behind the consumption of RuBP by Rubisco, and hence the limitation switches from Rubisco capacity to RuBP-regeneration capacity. The regeneration of RuBP by the Calvin-Benson cycle involves a number of enzymatic processes and requires reducing power as well as ATP. The former is supplied in the form of NADPH by the photosynthetic electron transport chain of the light reactions. The RuBP-regeneration capacity at subsaturating light, or at saturating light near the thermal optimum, typically reflects the electron transport capacity (*J*) in the leaf (von Caemmerer & Farquhar, 1981). At saturating light and at high CO_2 concentrations RuBP regeneration is controlled by the capacity of starch and sucrose synthesis from triose-phosphates to regenerate P_i for sustained ATP synthesis; these limitations have been termed TPU or P_i regeneration limitations (Sharkey, 1985; Cen & Sage, 2005). Such limitations are noted to be common in C_3 plants at saturating light, cooler temperatures and elevated CO_2 (Sharkey, 1985; Sage & Sharkey, 1987; Sage *et al.*, 1990; Harley & Sharkey, 1991).

Under conditions where the regeneration of RuBP directly depends upon the rate of electron transport, the rate of *A* is described by:

$$A_j = \frac{\left(C_c - \Gamma^*\right)J}{4C_c + 8\Gamma^*} - R_d \quad (3)$$

and when TPU capacity is limiting, *A* is described by

$$A_p = \frac{\left(C_c - \Gamma^*\right)3T_P}{C_c - \left(1+3\alpha\right)\Gamma^*} - R_d \quad (4)$$

where T_P is the rate of triose phosphate use (von Caemmerer, 2000). The photorespiratory cycle is responsible for a net release of phosphate in the chloroplast when some fraction $0 < \alpha < 1$ of the photorespiratory carbon is leaving the photorespiratory pathway to be used in amino acid synthesis. The phosphate normally used to regenerate PGA from glycerate is not needed for the fraction that remains outside the chloroplast as amino acids and is made available for photophosphorylation instead, stimulating *A* in the presence of photorespiration (Harley & Sharkey, 1991).

Depending on the limiting process at a given environmental condition, the actual value of *A* is determined by the minimum of the three rates A_c, A_j and A_p:

$$A = \min\left\{A_c, A_j, A_p\right\} \quad (5)$$

The sensitivity of *A* to a change in O_2 (*OS*), here from 210 to 20 mmol mol^{-1}, can be experimentally estimated as:

$$OS(A) = 1 - \frac{A_{210} + R_d}{A_{20} + R_d} \quad (6)$$

A_{210} and A_{20} are the net CO_2 assimilation rates at 210 and 20 mmol mol^{-1} O_2, respectively, and a common C_c. This measured value can now be compared to a modeled value, assuming one of the three limitations. Substituting Eqn. 2 into Eqn. 6, under the RuBP-saturated condition, $OS(A_c)$ can be modeled as:

$$OS(A_c) = 1 - \frac{A_{c210} + R_d}{A_{c20} + R_d} = 1 - \frac{\dfrac{\left(C_c - \Gamma^*_{210}\right)}{C_c + K_c\left(1 + O_{210}/K_o\right)}}{\dfrac{\left(C_c - \Gamma^*_{20}\right)}{C_c + K_c\left(1 + O_{20}/K_o\right)}} \quad (7)$$

This equation is now independent of one of the most critical, yet variable, parameters of the FvCB model, V_{cmax}. Potential inaccuracies in the remaining variables such as K_c and K_o are minimized, because they appear in both the numerator and the denominator. The same is true for potential inaccuracies in C_c due to assumed values for g_m. Over- or underestimations of g_m will over- or underestimate C_c in both the numerator and the denominator, which therefore has only a small impact on the measured values of *OS*. Similarly, for the RuBP-limited condition the model yields:

$$OS(A_j) = 1 - \frac{A_{j210} + R_d}{A_{j20} + R_d} = 1 - \beta \frac{\frac{\left(C_c - \Gamma^*_{210}\right)}{4C_c + 8\Gamma^*_{210}}}{\frac{\left(C_c - \Gamma^*_{20}\right)}{4C_c + 8\Gamma^*_{20}}} \quad (8)$$

In this case, the electron transport rate *J* does not fully cancel out, as J_{max} is not independent of the O_2 concentration, but remains as a constant described as $\beta = J_{\max 210} / J_{\max 20}$. The light-saturated value of J_{max} is higher at 21% O_2 than at 2% O_2, although the mechanism underlying this difference is not yet fully understood (Sharkey *et al.*, 1988; Laisk *et al.*, 2006; Yin *et al.*, 2009). Finally, the sensitivity of *A* to O_2 under a TPU limitation can be modeled with the following equation, which is independent of T_P:

$$OS(A_p) = 1 - \frac{A_{p210} + R_d}{A_{p20} + R_d} = 1 - \frac{\frac{\left(C_c - \Gamma^*_{210}\right)}{C_c - \left(1 + 3\alpha\right)\Gamma^*_{210}}}{\frac{\left(C_c - \Gamma^*_{20}\right)}{C_c - \left(1 + 3\alpha\right)\Gamma^*_{20}}} \quad (9)$$

Similarly, the sensitivity of *ETR*, estimated by pulse-amplitude modulated chlorophyll fluorescence, to O_2 can be measured as:

$$OS(ETR) = 1 - \frac{ETR_{210}}{ETR_{20}} \quad (10)$$

which can be compared to the modeled sensitivity. For the Rubisco and RuBP regeneration limitations we assumed that the electron transport rate is determined by NADPH consumption in photosynthesis and photorespiration, and therefore used $J / V_c = 4 + 8\Gamma^* / C_c$:

$$OS(ETR) = 1 - \frac{ETR_{210}}{ETR_{20}} = 1 - \frac{\left(A_{210} + R_d\right)\frac{4C_c + 8\Gamma^*_{210}}{C_c - \Gamma^*_{210}}}{\left(A_{20} + R_d\right)\frac{4C_c + 8\Gamma^*_{20}}{C_c - \Gamma^*_{20}}} \quad (11)$$

Substituting Eqns. 2, 3, or 4 for the gross CO_2 assimilation rate (A+R_d) in Eqn. 11 gives the oxygen sensitivities of *ETR* for the Rubisco and RuBP regeneration limitation scenario, respectively. For the TPU limitation we assumed that the regeneration of phosphate is limiting ATP synthesis (Labate & Leegood, 1988), but that the rate of ATP synthesis feeds back to NADPH production. In this case, linear electron transport through photosystem II can be taken as a good estimate for ATP production and therefore the equation above is also valid for a TPU limitation. For all three limitations we assume that alternative electron sinks are negligible. Should alternative electron sinks exist, however, they will likely occur at both O_2 concentrations. The effect on *OS* is therefore minimized, as *ETR* in both the numerator and denominator of the calculated *OS*(*ETR*) values will be affected in parallel.

Likewise, an increase in CO_2 concentration results in variable enhancements of *A*, depending on which process is limiting (Stitt, 1991). Analogous equations to Eqns. 6 to 11 can be employed to calculate the sensitivities of *A* and *ETR* to a change in CO_2 concentration (*CS*) (see Supporting Information, Notes S1). As the response of the sensitivities to O_2 and CO_2 differ qualitatively and quantitatively, the combination of all the sensitivities together can clarify, which limitation underlies CO_2 assimilation at any given environmental condition. Figure S1 outlines some of the processes underlying the different biochemical limitations of CO_2 uptake.

Materials and Methods

Plant material

Sweet potato plants (*Ipomoea batatas* (L.) Lam.) were grown in 20L pots in a greenhouse under natural light, supplemented by high-pressure sodium lamps to

maintain a minimum photon flux density during the photoperiod of 200 µmol photons m^{-2} s^{-1} (Cen & Sage, 2005). The plants were grown in sandy-loam soil and were watered regularly to avoid water stress. Fertilizer was supplied weekly as a 50:50 mixture of Miracle-Gro 24-10-10 All Purpose Plant Food and Miracle-Gro Evergreen Food (30-10-20) at the recommended dosage (22 mL of fertilizer salt per 6 L; Scotts Miracle-Gro; www.scotts.ca), and supplemented monthly with a 1 mM $MgSO_4$ and 6 mM $CaNO_3$ solution as found in a Johnson-Hoagland's solution (Epstein, 1972).

Gas exchange and chlorophyll fluorescence

Leaf gas exchange and fluorescence for the CO_2 responses were measured with an open-path gas exchange system (LI-6400; Li-Cor, Lincoln, NE, USA), equipped with a leaf chamber fluorometer (6400-40; Li-Cor, Lincoln, NE, USA). The response of *A* to intercellular CO_2 concentrations (C_i) was measured on young, fully expanded leaves at two O_2 concentrations of 210 and 20 mmol mol^{-1}. Photosynthetically active radiation (PAR) was set to 1500 µmol photons m^{-2} s^{-1} at constant leaf temperatures of 15°, 20°, 25°, 30°, 35° and 40°C. Leaf vapor pressure deficit (VPD) was kept between 1 and 1.5 kPa, except for at 35° and 40°C, at which it was around 2.5 and 3.5 kPa, respectively.

Temperature responses of net CO_2 assimilation rates were measured with a null-balance gas exchange system as described by Pittermann and Sage (2000), fitted with a custom-build chamber and a PAM 2100 (Heinz Walz, Effeltrich, Germany) for concomitant chlorophyll fluorescence measurements and a white LED light source for illumination (PSI, Brno, Czech Republic). The measurements were performed on a leaf area of approximately 20 cm^2, which was achieved by trimming the leaves to the desired size on the day before the measurement. Temperature response measurements began at 25°C and the temperature was decreased stepwise to 10°C with an acclimation time of 15-20 minutes at each temperature. The leaves were then returned to 25°C for 30 minutes, after which the temperature was stepwise increased to 45°C. At each leaf temperature, gas exchange and chlorophyll fluorescence parameters were measured at 21% and 2% O_2 in random order. Measurements were performed on separate leaves for

light intensities of 250 and 900 µmol photons m^{-2} s^{-1}, and CO_2 concentrations of 380 and 1500 µmol mol^{-1}.

Chlorophyll fluorescence was used to measure steady state (F_s), maximum (F_m') and minimum (F_o') fluorescence yields concomitantly with gas exchange. For the temperature response measurements F_o' was calculated according to Oxborough and Baker (1997). From these parameters the effective quantum yield was estimated as $\Phi_{II} = \left(F_m' - F_s\right) / F_m'$ (Genty *et al.*, 1989), from which the photosynthetic electron transport rate was calculated as $ETR = \Phi_{II}$ x 0.84 x 0.5 x PAR. The fraction of PSII reaction centers in a closed state, used as an indication of excitation pressure, was estimated as $1 - qP = 1 - \left(F_m' - F_s\right) / \left(F_m' - F_o'\right)$ (Huner *et al.*, 1996). *NPQ* was calculated as $F_m / F_m' - 1$ according to Bilger and Björkman (1990), with the maximum fluorescence yield F_m measured after 30 minutes of dark acclimation at 25°C before starting the temperature response in the light.

Mitochondrial respiration in the light (R_d) was estimated by the Kok method from the response of *A* to PAR at leaf temperatures of 15°, 20°, 25°, 30°, 35° and 40°C (Kok, 1948). These measurements were performed with a 6 cm^2 chamber with a red-blue LED light source (6400-02B; Li-Cor, Lincoln, NE, USA) attached to the LI-6400 gas exchange system to minimize diffusion leaks. The data were corrected for respiratory CO_2 released under the gasket according to Pons and Welschen (2002).

O_2 and CO_2 sensitivity measurements

We estimated chloroplastic CO_2 concentrations (C_c) from the measured C_i values by assuming a g_m of 0.5 mol CO_2 m^{-2} s^{-1} bar^{-1} at 25°C using the relation $C_c = C_i - A / g_m$. For temperatures other than 25°C, we adjusted g_m with an Arrhenius-type temperature dependency scaling constant (*c*) of 11.81 and an activation energy (ΔH_a) of 29.17 kJ mol^{-1} (Scafaro *et al.*, 2011). To obtain values of *A*, *ETR* and 1-qP for the same value of C_c at different O_2 concentrations, individual C_c response curves were smoothed with a quadratic Savitzky-Golay function and interpolated to 10 µmol mol^{-1} C_c intervals using the OriginPro software package (OriginLab Corporation, Northampton, MA, USA).

Temperature responses were treated similarly to obtain values at common temperatures for the calculation of O_2 and CO_2 sensitivities. Figure S2 shows sample A/C_c and ETR/C_c response curves treated this way. Maximum values of the ETR/C_c curves were determined at 21% and 2% O_2 to approximate β and estimate the effect of the O_2 concentration on J. A value of α = 0.30 was used for the sensitivity calculations involving a TPU limitation, which was obtained by fitting Eqn. (9) to our data at 25°C. We have applied this value of α to all temperatures, since an accurate fit was not possible at high temperatures due to a lack of TPU limitation. Using different values of α affects the goodness of the fit, but does not affect the conclusions drawn from the analysis (see Fig. S3). We used the seven sets of Rubisco kinetic parameters (K_c, K_o and Γ^*) outlined in Fig. 1 to calculate *OS* and *CS*, consisting of *Nicotiana tabacum* (Bernacchi *et al.*, 2001), *Spinacia oleracea* (Jordan & Ogren, 1984) and *Atriplex glabriuscula* with Γ^* from *S. oleracea* (Badger & Collatz, 1977; Brooks & Farquhar, 1985), as described in Medlyn *et al.* (2002), as well as *N. tabacum* (Bernacchi *et al.*, 2002), a 'model plant' (von Caemmerer, 2000), *Arabidopsis thaliana*, and *N. tabacum* (Walker *et al.*, 2013).

Results

Figure 1 shows the variability between studies and species in the thermal response of four major inputs into the FvCB model (Γ^*, K_m, V_{cmax}, and J_{max}). Using these inputs, responses of *OS* and *CS* to chloroplast CO_2 concentration were first modeled assuming A is limited by Rubisco carboxylation capacity (A_c), RuBP regeneration capacity (A_j) or TPU capacity (A_p; Fig. 2). Despite the large variation in the values of the input parameters (Fig. 1), the *OS* and *CS* responses to C_c were similar for a given biochemical limitation (Fig. 2), demonstrating the ability of the *OS* and *CS* methodology to minimize impacts of parameter variation. We then compared modeled with measured sensitivities, since correspondence can identify the underlying biochemical limitations controlling A. For C_c values between 200 and 400 µmol mol^{-1}, the measured data correspond to modeled sensitivities for electron transport limitation in each of the four panels in Fig. 2,

providing solid support that electron transport capacity limits *A* at this range of CO_2. At C_c values below 100 µmol mol^{-1}, *OS*(A_c) and *OS*(A_j) are both similar to the observed *OS*(*A*) response (Fig. 2a-b); however, *CS*(ETR_c) and *CS*(ETR_j) are distinctly different, with the measured values of *CS*(*ETR*) only aligning with *CS*(ETR_c) (Fig. 2c-d). Since the correspondence has to be simultaneously present in all four scenarios shown in panels a-d of Fig. 2, we can therefore conclude that below 100 µmol CO_2 mol^{-1} measured *OS*(*A*) follows the modeled values of *OS*(A_c) rather than *OS*(A_j); a Rubisco capacity limitation is therefore present. Above 550 µmol mol^{-1}, the modeled sensitivities assuming a TPU limitation best fit the observed responses, indicating TPU capacity limits *A* at elevated CO_2. At CO_2 concentrations where one limitation transitions into the next, values of measured *OS* and *CS* are typically intermediate between two modeled limitations (hatched areas in Fig. 2). Under these conditions the underlying limitation differs between the two O_2 concentrations when measuring *OS* (or CO_2 concentrations when measuring *CS*). A more detailed description of this situation is provided in the Supporting Information, Notes S2.

To further support our evaluation of the conditions, under which RuBP regeneration is limiting *A*, we assessed C_c response curves of *ETR* relative to its maximum value and the C_c response of excitation pressure (1-qP) in leaves. Relative *ETR* values are expected to be near 1 when *ETR* is limiting (indicated as green shaded regions of the responses in Fig. 3, defined here as being within 5% of the absolute maximum value of *ETR*), but decline as limitations elsewhere feedback onto electron transport capacity. With increasing temperature, the C_c range where relative *ETR* is near 1 expands and shifts to higher CO_2 concentrations. A similar pattern emerges from the response of 1-qP to C_c (Fig. 4). The term 1-qP is a measure of the imbalance between the energy supply from light and the energy consumption by RuBP regeneration. Its values should be minimal when the PSII turnover rate limits *ETR*, and increase when rates of NADPH consumption are lower than potential rates of NADPH production feedback on the linear electron transport rate, as seen under the Rubisco and TPU limitations. The minimum values of 1-qP (taken as the values falling into the lowest 1% and indicated in

388 green; Fig. 4) coincide well with the ranges of CO_2 concentrations where relative *ETR* is
389 approximately 1 (Fig. 3). These results also agree with the CO_2 ranges determined to be
390 electron transport limited from the analysis of *OS* and *CS* (Fig. 2).

391 Figure 5 shows the pattern of limitations for the A/C_c responses at six different
392 temperatures predicted from *OS* and *CS*, as well as the A/C_c responses at 21% and 2% O_2
393 used to derive these limitations. In all cases a Rubisco limitation at low CO_2
394 concentrations transitions to a RuBP-regeneration limitation at mid-level CO_2
395 concentrations, which is followed by a TPU limitation at high CO_2 concentrations. This
396 agrees with the order that is dictated by the FvCB model (Gu *et al.*, 2010). Similar to
397 what was observed with the maximum rates of *ETR* and 1-qP, the C_c concentration at
398 which one limitation transitions into the next is increasing slightly with increasing
399 temperature up to 35°C. Increasing the temperature from 35° to 40°C more than
400 doubles the C_c range where A_c is limiting (Fig. 5). The TPU limitation at 35°C was
401 restricted to only the highest C_c and was not apparent at any CO_2 concentration at 40°C.

402 The thermal responses of gross CO_2 assimilation ($A+R_d$), *ETR*, and *NPQ* at a sub-
403 saturating light intensity of 250 µmol m^{-2} s^{-1} were examined to further evaluate RuBP
404 regeneration limitations (Fig. 6). At a CO_2 concentration of 380 µmol mol^{-1} $A+R_d$ declines
405 above 25°C, whereas at a CO_2 concentration of 1500 µmol mol^{-1} no substantial decline
406 was observed between 25° and 43°C (Fig. 6a). The *ETR* stayed constant between 20° and
407 35°C and values were equivalent for all CO_2 and O_2 combinations. *ETR* declines above
408 35°C at 380 µmol mol^{-1} CO_2 / 2% O_2, but does not decrease until above 40°C when
409 measured at 380 µmol mol^{-1} CO_2 / 21% O_2, and 43°C at 1500 µmol mol^{-1} and 21%,
410 respectively (indicated by the arrows). The non-photochemical energy dissipation
411 parameter *NPQ*, shown in Fig. 6c, describes in relative terms how much of the absorbed
412 light is quenched as heat before PS II and therefore does not contribute to *ETR*. *NPQ*
413 stays low until much higher temperatures when the leaf is exposed to 1500 µmol mol^{-1}
414 CO_2 as compared to 380 µmol mol^{-1} CO_2 (at either 21% or 2% O_2). Combined, these two
415 observations demonstrate that the plant maintains a constant RuBP-regeneration
416 capacity up to at least 43°C given sufficient electron acceptors for RuBP consumption.

At a light intensity of 900 µmol m^{-2} s^{-1}, *A* is insensitive to changes in photorespiration caused by changes in CO_2 or O_2 concentrations at temperatures below 22°C, indicating a TPU limitation (Fig. 7a). At 1500 µmol CO_2 mol^{-1} air, *A* is insensitive to change in O_2 concentration up to near 32°C. Similarly, at 2% O_2, *A* does not increase with a step change in CO_2 from 380 to 1500 µmol mol^{-1} at temperatures below 32°C, consistent with a TPU limitation. However, at both oxygen concentrations *A* is stimulated by this increase in CO_2 concentration at 32°C and above (Fig. 7a). Under non-photorespiratory conditions, Rubisco uses RuBP for carboxylation rather than oxygenation reactions. Therefore, if *A* can be increased at 2% O_2 by increasing the CO_2 concentration, it means that the rate of RuBP regeneration can be increased to match an increased rate of RuBP consumption by Rubisco. When Rubisco is limiting in C_3 plants, CO_2 increase typically stimulates the carboxylation rate in its role as a substrate, which in turn can allow the RuBP regeneration rate to increase. These results demonstrate that at 2% O_2, RuBP regeneration capacity is not a limitation for CO_2 uptake at high temperatures.

An increase in CO_2 concentration decreases *ETR* at low temperatures, while at high temperatures *ETR* is higher at 1500 than at 380 µmol mol^{-1} CO_2 (Fig. 7b). At 2% O_2, *ETR* starts to decrease above 34°C at 380 µmol mol^{-1} CO_2, whereas at 1500 µmol mol^{-1} CO_2 it does not decrease until 42°C (Fig. 7b). This result is mirrored in 1-qP, which starts to increase from a minimum value at 34°C, 40°C and 43°C under the 380/2%, 380/21% and 1500/2% conditions, respectively (Fig. 7c). Again, the pattern of *ETR* at the four different gas mixes indicates that RuBP-regeneration is not limiting at high temperatures under 380 µmol mol^{-1} CO_2 and 21% O_2.

Temperature responses of *OS* and *CS* were calculated using data presented in Fig. 7. At a CO_2 concentration of 380 µmol mol^{-1} the measured *OS*(*A*) aligns with the modeled values of *OS*(A_p) below 17°C, above which it transitions to values expected under a A_j or A_c-limitation (Fig. 8a). *OS*(*ETR*) transitions from a A_p-limitation below 20°C to a A_j-limitation between 25° and 30°C, above which it most closely aligns with the A_c-limitation (Fig. 8b). Similarly, at 21% O_2, the *CS*(*A*) calculated from a shift in CO_2

concentration from 380 to 1500 µmol mol^{-1} indicates a transition from a A_p to a A_j-limitation between 30° and 40°C and then to a A_c-limitation above 40°C (Fig. 8c). Measured values of *CS*(*A*) at 2% O_2 closely approximate modeled values of *CS*(A_p) below 25°C, and are equivalent to *CS*(A_j) at 30° before rising towards modeled *CS*(A_c) above 40°C (Fig. 8d). Equivalent figures for a light intensity of 250 µmol m^{-2} s^{-1} are displayed in the Supplemental Information (Fig. S4). Here, measured values intermediate between two limitations can be assigned to one single limitation: values intermediate between *CS*(A_c) and *CS*(A_j) have to be viewed as A_c-limited at 380 µmol mol^{-1}, whereas values intermediate between *CS*(A_j) and *CS*(A_p) have to be viewed as A_j-limited, which follows from the order of limitations along a CO_2 gradient dictated by the FvCB model (Gu *et al.*, 2010; also see Supporting Information, Notes S2). Similarly, intermediate values of *OS* can be assigned to one single limitation due to the order of limitations dictated along an O_2 gradient. At 2% O_2 we can exclude the masking effect of photorespiration and attribute a decline in *A* directly to a decrease in the RuBP consumption capacity rather than an increase in photorespiration. This unambiguously demonstrates that the rate of Rubisco carboxylation is sensitive to temperatures above around 35°C.

Figure 9 integrates the observations above into a 3D response of the biochemical limitations of *A* as a function of CO_2 and temperature. At low temperatures, a TPU limitation can be observed as the yellow colored portion of the response surface at elevated C_c values. The CO_2 concentration where *A* is TPU limited declines to near 300 µmol mol^{-1} at 15°C. At high temperatures TPU was not found to be limiting even at the highest CO_2 concentrations. Rubisco controls *A* at low C_c throughout the temperature range measured. The range of CO_2 concentrations, in which Rubisco is limiting expands with increasing temperature from below 120 µmol mol^{-1} CO_2 at 15°C to near 280 µmol mol^{-1} CO_2 at 35°C. Above 35°C there is a steep increase in the CO_2 concentration below which Rubisco is limiting, coinciding with a sharp drop in *A*. Electron transport is limiting at the interface between the Rubisco and TPU limitations and is the dominating limitation over *A* below the thermal optimum at a measuring light intensity of 1500 µmol photons m^{-2} s^{-1} and C_c values corresponding to the current atmospheric CO_2

concentrations outside the leaf (C_a). Above the thermal optimum Rubisco is limiting at ambient C_a (Fig. 9).

Discussion

Using revised gas exchange and chlorophyll fluorescence analysis of O_2 and CO_2 sensitivity of *A* and *ETR*, we have generated for the first time a three-dimensional landscape of photosynthetic limitations in C_3 plants as a function of CO_2 and temperature. Large differences in the parameters entered into the model had only a minor effect on the predicted *OS* and *CS* values, demonstrating that the CO_2 response of *OS* and *CS* is more dependent on the properties of the FvCB model itself rather than the selected inputs. Because our method provides an assessment of the biochemical limitations that is entirely independent of the variable parameters and largely independent of the values chosen for the fixed parameters, the *OS* and *CS* analysis minimizes the vulnerability of the model predictions to mismatches between assumed and actual input values. As such, an *OS* and *CS* analysis can provide a robust, complimentary evaluation of photosynthetic limitations when coupled with FvCB simulations.

Our analysis of sweet potato gas exchange supports prior observations in the literature, namely that *A* is limited by TPU at cooler temperatures and elevated CO_2, and that TPU capacity can limit *A* at current atmospheric CO_2 concentrations below about 20°C. We also observed that Rubisco capacity limits *A* across a broad range of temperatures at low CO_2 (below a C_c of 150 µmol mol^{-1}). These observations demonstrate an ability of our analysis to replicate well-described observations. Our analysis clarifies two areas of long-standing uncertainty that have been debated in the recent literature. First, under high light conditions, RuBP regeneration capacity is the effective limitation over *A* at the photosynthetic thermal optimum and CO_2 concentrations from 380 to above 1000 µmol mol^{-1}, contrasting prior studies that implicate Rubisco as a leading limitation at the thermal optimum (e.g. Cen & Sage,

2005). This conclusion is supported by the *OS* and *CS* analysis, as well as the response of *ETR* and 1-qP to changes in CO_2 concentration and temperature.

Second, the decline of *A* above the thermal optimum has been argued to either reflect a limitation of the capacity to regenerate RuBP, or heat-induced lability of Rubisco activase (Salvucci & Crafts-Brandner, 2004; Schrader *et al.*, 2004; Wise *et al.*, 2004; Cen & Sage, 2005; Hikosaka *et al.*, 2006; Makino & Sage, 2007; Sage & Kubien, 2007). Here, the evidence supports a limitation in Rubisco capacity to consume RuBP above the thermal optimum, as shown by the *OS* and *CS* analysis and the thermal stability of the RuBP regeneration capacity at low light. In addition, at high temperatures we have shown a strong *CS* in the absence of photorespiration, which contradicts a limitation in the supply of RuBP. This observation demonstrates the heat lability of Rubisco capacity under non-photorespiratory conditions, which is a response that likely remains unchanged under photorespiratory conditions. The limitation in Rubisco capacity is predicted to extend to relatively high CO_2 levels (2x ambient) at temperatures near 40°C, and to concentrations as high as 1500 µmol mol^{-1} at temperatures around 45°C, as demonstrated by the results of *CS*(*A*) at 21% O_2 (Fig. 8c). Our predictions also contrast model outcomes with commonly used parameters that frequently place a Rubisco or RuBP regeneration limitation at low and a TPU limitation at high temperatures (see e.g. *A*/*T* model parameterization in Bernacchi *et al*. 2013).

Our results show that above 35°C, *A* has to be limited either by the supply of Rubisco's other substrate, CO_2, or by a decrease in V_{cmax}. Mesophyll conductance, and therefore the supply of CO_2, tends to increase with temperature, ruling out the first possibility (von Caemmerer & Evans, 2015; but see Bernacchi *et al*. 2002 for a decline in g_m at high temperatures). Loss of Rubisco capacity by direct thermal inactivation of the active site is also unlikely given V_{cmax} of fully activated enzyme increases with temperature to above 50°C (Laidler & Peterman, 1979; Crafts-Brandner & Salvucci, 2000). *In vivo*, Rubisco is kept in its active state by Rubisco activase, a AAA+ chaperone that removes RuBP and other sugar phosphates that tightly bind to decarbamylated Rubisco catalytic sites (Portis, 2003). A decline of *A* at temperatures above 35°C is

consistent with the heat lability of Rubisco activase and its activity failing to keep pace with the deactivation of Rubisco at those temperatures (Law & Crafts-Brandner, 1999; Crafts-Brandner & Salvucci, 2000; Salvucci & Crafts-Brandner, 2004). This cause of Rubisco deactivation was disputed previously, because earlier studies did not rule out the possibility that the activase lability occurred in response to limitations in electron transport capacity (Sage & Kubien, 2007). Cen and Sage (2005) attributed a deactivation of Rubisco observed at high temperatures to a regulatory feedback on Rubisco from limitations in TPU and RuBP regeneration capacity. Because our sweet potato plants and growth conditions were identical to those used in their study, we conclude that the differences between the respective predicted limitations are not biological, but reflect different analytical approaches. This highlights the risks of selecting various kinetic parameters from the literature to obtain a good fit of the model to the data, as was done by Cen and Sage (2005), and emphasizes the need for analytical approaches such as *OS* and *CS* that are insensitive to modeled inputs not derived from the species under study.

Implications for fitting the FvCB model to measured data

Estimating parameters of the FvCB model by fitting the model to A/C_i curves is influenced by how an observer assigns individual measurements to different segments fitted by the model. Without *a priory* knowledge of where the cut-off point between data points used to fit the Rubisco-limited function and points used to fit the RuBP-regeneration limited function, an incorrect assignment of measured values to the limiting processes can have a large impact on estimated parameters, such as V_{cmax}, J and R_d (Manter & Kerrigan, 2004; Dubois *et al.*, 2007). TPU limitation is often assumed to only occur at very high CO_2 concentrations or is neglected altogether, leaving TPU-limited measurements assigned to the RuBP-limited segment and thus often erroneously influencing estimates of J. This study shows that the range of where CO_2 assimilation is TPU limited may be significant and, especially at lower temperatures, should not be overlooked. Depending on growth and measurement conditions, any one

of the limitations might be missing, e.g. an RuBP regeneration limitation can control *A* at all C_i at low light (Sharkey *et al.*, 2007). Any fitting approach to determine the FvCB model parameters can now be supported by the presented O_2 and CO_2 sensitivity measurements, which can objectively assign data points to specific segments to be fitted by the individual functions and thereby complement the chosen fitting approach.

Similarly, choosing inappropriate temperatures responses for model parameters can lead to assigning functions of the FvCB model to temperature ranges, over which the assigned limiting process is not actually limiting, causing problems when modeling *A*. Our analysis of *OS* and *CS* can be used to avoid these issues. For sweet potato we demonstrate a Rubisco limitation at ambient C_a and higher temperatures (Fig. 9); any model fit that results e.g. in a TPU limitation for this region implies a problem with that particular parameter set and its temperature response used in the FvCB model. Mesophyll conductance is likely the source of many errors in modeling related to incorrectly assigning biochemical limitations, as the temperature response of g_m is highly variable between species and typically not derived from data measured on the plant of study (von Caemmerer & Evans, 2015). Assumed values of g_m also affect our calculations of *OS* and *CS* and it is preferable to have them directly measured. Similar to the impact of the fixed parameters, however, the parameterization of *OS* and *CS* as a ratio minimizes the effect of uncertainties in g_m and setting g_m to low values and even infinite does not change the overall conclusion drawn from the model (Fig. S5).

Choosing strategies to improve crop yield by increasing photosynthetic CO_2 uptake

Providing sufficient food for the world's growing population is one of the big challenges humanity will face in the near future. While there is not always a strong link between photosynthetic CO_2 uptake and improved crop yield, in general it seems to be beneficial to increase *A* to obtain a higher plant biomass (Long *et al.*, 2006). Many strategies to increase *A* have been proposed, from altering Rubisco kinetic properties to reduce photorespiration, over improving the thermotolerance of Rubisco activase, the CO_2 diffusion into the chloroplast, and boosting photosynthetic light use efficiency, to

enhancing the capacity of carbon utilization (discussed, e.g., in Ort *et al.*, 2011; Betti *et al.*, 2016; Yamori *et al.*, 2016). Many of these approaches will work better under some environmental conditions than others, and our results will help narrow down strategies that will be successful. For example, one might want to improve the capacity for TPU to make plants assimilate more CO_2 in cold climates, manipulate aspects that result in higher V_{cmax} to enhance plant performance in hot growth environments, or improve light harvesting and photosynthetic electron transport in plants that grow close to their photosynthetic optimum. As climate is becoming more unpredictable and volatile, understanding the photosynthetic limitations for a given environmental condition becomes highly valuable to address various limitations and produce climate-resilient plants.

Benefits to modeling photosynthesis from the leaf level to the global scale under future climates

By providing a robust assessment of the biochemical limitations controlling *A*, the O_2 and CO_2 sensitivity approach used here overcomes the vulnerability to mismatches between assumed and actual input values for a given species, and thus provides an independent check of the predictions arising from FvCB simulations. Small errors in photosynthesis estimates on the leaf scale can result in large uncertainties of global estimates of carbon uptake, which makes the response of the terrestrial carbon cycle to changes in CO_2 concentration and temperature one of the least understood processes in earth system models (Rogers, 2014). Understanding which biochemical process is limiting for a given environmental condition is an important step towards improving the representation of photosynthetic processes in these models. For example, assuming a Rubisco limitation at high temperatures will predict an increase in *A* with rising [CO_2], whereas assuming a TPU limitation will not. Assigning the biochemical limitation correctly will therefore increase the confidence in the accuracy of the used parameter values to predict *A* for situations for which direct measurements may not be available,

such as when modeling future climates. The analysis of *OS* and *CS* provides a useful tool to do just that.

Acknowledgements

This work was funded by an NSERC Discovery and an NSERC Accelerator grant to R.F.S. F.A.B. is supported by the ARC Centre of Excellence for Translational Photosynthesis.

Author contributions

F.A.B. and R.F.S. planned and designed the research. F.A.B. performed the experiments and analyzed the data. F.A.B. and R.F.S. wrote the manuscript.

Literature

Badger MR, Collatz GJ. 1977. Studies on the kinetic mechanism of ribulose-1,5-bisphosphate carboxylase and oxygenase reactions, with particular reference to the effect of temperature on kinetic parameters. *Carnegie Institution Year Book* **76**: 355-361.

Bernacchi CJ, Bagley JE, Serbin SP, Ruiz-Vera UM, Rosenthal DM, Vanloocke A. 2013. Modelling C_3 photosynthesis from the chloroplast to the ecosystem. *Plant, Cell & Environment* **36**(9): 1641-1657.

Bernacchi CJ, Portis AR, Nakano H, von Caemmerer S, Long SP. 2002. Temperature response of mesophyll conductance. Implications for the determination of Rubisco enzyme kinetics and for limitations to photosynthesis in vivo. *Plant Physiology* **130**(4): 1992-1998.

Bernacchi CJ, Singsaas EL, Pimentel C, Portis AR, Long SP. 2001. Improved temperature response functions for models of Rubisco-limited photosynthesis. *Plant, Cell & Environment* **24**(2): 253-259.

Betti M, Bauwe H, Busch FA, Fernie AR, Keech O, Levey M, Ort DR, Parry MAJ, Sage R, Timm S, Walker B, Weber APM. 2016. Manipulating photorespiration to increase plant productivity: recent advances and perspectives for crop improvement. *Journal of Experimental Botany* **67**(10): 2977-2988.

Bilger W, Björkman O. 1990. Role of the Xanthophyll Cycle in Photoprotection Elucidated by Measurements of Light-Induced Absorbency Changes, Fluorescence and Photosynthesis in Leaves of *Hedera canariensis*. *Photosynthesis Research* **25**(3): 173-185.

Booth BBB, Jones CD, Collins M, Totterdell IJ, Cox PM, Sitch S, Huntingford C, Betts RA, Harris GR, Lloyd J. 2012. High sensitivity of future global warming to land carbon cycle processes. *Environmental Research Letters* **7**(2): 024002.

Brooks A, Farquhar GD. 1985. Effect of temperature on the CO_2/O_2 specificity of ribulose-1,5-bisphosphate carboxylase oxygenase and the rate of respiration in

the light - Estimates from gas-exchange measurements on spinach. *Planta* **165**(3): 397-406.

Cen YP, Sage RF. 2005. The regulation of rubisco activity in response to variation in temperature and atmospheric CO_2 partial pressure in sweet potato. *Plant Physiology* **139**(2): 979-990.

Crafts-Brandner SJ, Salvucci ME. 2000. Rubisco activase constrains the photosynthetic potential of leaves at high temperature and CO_2. *Proceedings of the National Academy of Sciences of the United States of America* **97**(24): 13430-13435.

Dubois JJB, Fiscus EL, Booker FL, Flowers MD, Reid CD. 2007. Optimizing the statistical estimation of the parameters of the Farquhar-von Caemmerer-Berry model of photosynthesis. *New Phytologist* **176**: 402-414.

Ensminger I, Busch F, Hüner NPA. 2006. Photostasis and cold acclimation: sensing low temperature through photosynthesis. *Physiologia Plantarum* **126**(1): 28-44.

Epstein E. 1972. *Mineral nutrition of plants: principles and perspectives*. New York: John Wiley and Sons, Inc.

Ethier GJ, Livingston NJ. 2004. On the need to incorporate sensitivity to CO_2 transfer conductance into the Farquhar-von Caemmerer-Berry leaf photosynthesis model. *Plant, Cell & Environment* **27**(2): 137-153.

Evans JR, von Caemmerer S. 2013. Temperature response of carbon isotope discrimination and mesophyll conductance in tobacco. *Plant, Cell & Environment* **36**(4): 745-756.

Farquhar GD, von Caemmerer S, Berry JA. 1980. A biochemical model of photosynthetic CO_2 assimilation in leaves of C_3 species. *Planta* **149**(1): 78-90.

Farquhar GD, von Caemmerer S, Berry JA. 2001. Models of photosynthesis. *Plant Physiology* **125**(1): 42-45.

Flexas J, Carriquí M, Coopman RE, Gago J, Galmés J, Martorell S, Morales F, Diaz-Espejo A. 2014. Stomatal and mesophyll conductances to CO_2 in different plant groups: Underrated factors for predicting leaf photosynthesis responses to climate change? *Plant Science* **226**(0): 41-48.

Friedlingstein P, Cox P, Betts R, Bopp L, von Bloh W, Brovkin V, Cadule P, Doney S, Eby M, Fung I, Bala G, John J, Jones C, Joos F, Kato T, Kawamiya M, Knorr W, Lindsay K, Matthews HD, Raddatz T, Rayner P, Reick C, Roeckner E, Schnitzler KG, Schnur R, Strassmann K, Weaver AJ, Yoshikawa C, Zeng N. 2006. Climate–carbon cycle feedback analysis: results from the C^4MIP model intercomparison. *Journal of Climate* **19**(14): 3337-3353.

Galmés J, Hermida-Carrera C, Laanisto L, Niinemets Ü. 2016. A compendium of temperature responses of Rubisco kinetic traits: variability among and within photosynthetic groups and impacts on photosynthesis modeling. *Journal of Experimental Botany* **67**(17): 5067-5091.

Gandin A, Koteyeva NK, Voznesenskaya EV, Edwards GE, Cousins AB. 2014. The acclimation of photosynthesis and respiration to temperature in the C_3–C_4 intermediate *Salsola divaricata*: induction of high respiratory CO_2 release under low temperature. *Plant, Cell & Environment* **37**(11): 2601-2612.

Genty B, Briantais JM, Baker NR. 1989. The Relationship between the Quantum Yield of Photosynthetic Electron-Transport and Quenching of Chlorophyll Fluorescence. *Biochimica et Biophysica Acta* **990**(1): 87-92.

Gu LH, Pallardy SG, Tu K, Law BE, Wullschleger SD. 2010. Reliable estimation of biochemical parameters from C_3 leaf photosynthesis-intercellular carbon dioxide response curves. *Plant Cell and Environment* **33**(11): 1852-1874.

Harley PC, Sharkey TD. 1991. An improved model of C_3 photosynthesis at high CO_2: Reversed O_2 sensitivity explained by lack of glycerate reentry into the chloroplast. *Photosynthesis Research* **27**(3): 169-178.

Harley PC, Thomas RB, Reynolds JF, Strain BR. 1992. Modeling Photosynthesis of Cotton Grown in Elevated CO_2. *Plant Cell and Environment* **15**(3): 271-282.

Hermida-Carrera C, Kapralov MV, Galmés J. 2016. Rubisco catalytic properties and temperature response in crops. *Plant Physiology* **171**(4): 2549-2561.

Hikosaka K, Ishikawa K, Borjigidai A, Muller O, Onoda Y. 2006. Temperature acclimation of photosynthesis: mechanisms involved in the changes in

temperature dependence of photosynthetic rate. *Journal of Experimental Botany* **57**(2): 291-302.

Huner NPA, Maxwell DP, Gray GR, Savitch LV, Krol M, Ivanov AG, Falk S. 1996. Sensing environmental temperature change through imbalances between energy supply and energy consumption: Redox state of photosystem II. *Physiologia Plantarum* **98**(2): 358-364.

Jordan DB, Ogren WL. 1984. The CO_2/O_2 specificity of ribulose 1,5-bisphosphate carboxylase oxygenase - Dependence on ribulosebisphosphate concentration, pH and temperature. *Planta* **161**(4): 308-313.

Kattge J, Knorr W. 2007. Temperature acclimation in a biochemical model of photosynthesis: a reanalysis of data from 36 species. *Plant, Cell & Environment* **30**(9): 1176-1190.

Kok B. 1948. A critical consideration of the quantum yield of *Chlorella*-photosynthesis. *Enzymologia* **13**: 1-56.

Labate C, Leegood R. 1988. Limitation of photosynthesis by changes in temperature. *Planta* **173**(4): 519-527.

Laidler KJ, Peterman BF. 1979. Temperature effects in enzyme kinetics. *Methods in Enzymology* **63**: 234-257.

Laisk A, Eichelmann H, Oja V, Rasulov B, Ramma H. 2006. Photosystem II cycle and alternative electron flow in leaves. *Plant and Cell Physiology* **47**(7): 972-983.

Law RD, Crafts-Brandner SJ. 1999. Inhibition and acclimation of photosynthesis to heat stress is closely correlated with activation of ribulose-1,5-bisphosphate carboxylase/oxygenase. *Plant Physiology* **120**(1): 173-182.

Long SP, Zhu X-G, Naidu SL, Ort DR. 2006. Can improvement in photosynthesis increase crop yields? *Plant, Cell & Environment* **29**(3): 315-330.

Makino A, Sage RF. 2007. Temperature response of photosynthesis in transgenic rice transformed with 'sense' or 'antisense' rbcS. *Plant and Cell Physiology* **48**: 1472-1483.

744 **Manter DK, Kerrigan J. 2004.** A/Ci curve analysis across a range of woody plant species:
745 influence of regression analysis parameters and mesophyll conductance. *Journal*
746 *of Experimental Botany* **55**(408): 2581-2588.
747 **Massad R-S, Tuzet A, Bethenod O. 2007.** The effect of temperature on C_4-type leaf
748 photosynthesis parameters. *Plant, Cell & Environment* **30**(9): 1191-1204.
749 **Medlyn BE, Dreyer E, Ellsworth D, Forstreuter M, Harley PC, Kirschbaum MUF, Le Roux**
750 **X, Montpied P, Strassemeyer J, Walcroft A, Wang K, Loustau D. 2002.**
751 Temperature response of parameters of a biochemically based model of
752 photosynthesis. II. A review of experimental data. *Plant, Cell & Environment*
753 **25**(9): 1167-1179.
754 **Orr D, Alcântara A, Kapralov MV, Andralojc J, Carmo-Silva E, Parry MAJ. 2016.**
755 Surveying Rubisco diversity and temperature response to improve crop
756 photosynthetic efficiency. *Plant Physiology*. doi:10.1104/pp.16.00750
757 **Ort DR, Zhu X, Melis A. 2011.** Optimizing antenna size to maximize photosynthetic
758 efficiency. *Plant Physiology* **155**(1): 79-85.
759 **Oxborough K, Baker NR. 1997.** Resolving chlorophyll a fluorescence images of
760 photosynthetic efficiency into photochemical and non-photochemical
761 components - calculation of qP and Fv'/Fm' without measuring Fo'.
762 *Photosynthesis Research* **54**(2): 135-142.
763 **Pittermann J, Sage RF. 2000.** Photosynthetic performance at low temperature of
764 *Bouteloua gracilis* Lag., a high-altitude C_4 grass from the Rocky Mountains, USA.
765 *Plant, Cell & Environment* **23**(8): 811-823.
766 **Pons TL, Flexas J, von Caemmerer S, Evans JR, Genty B, Ribas-Carbo M, Brugnoli E.**
767 **2009.** Estimating mesophyll conductance to CO_2: methodology, potential errors,
768 and recommendations. *Journal of Experimental Botany* **60**(8): 2217-2234.
769 **Pons TL, Welschen RAM. 2002.** Overestimation of respiration rates in commercially
770 available clamp-on leaf chambers. Complications with measurement of net
771 photosynthesis. *Plant, Cell & Environment* **25**(10): 1367-1372.

Portis AR. 2003. Rubisco activase – Rubisco's catalytic chaperone. *Photosynthesis Research* **75**(1): 11-27.

Prentice IC, Bondeau A, Cramer W, Harrison SP, Hickler T, Lucht W, Sitch S, Smith B, Sykes MT 2007. Dynamic global vegetation modeling: quantifying terrestrial ecosystem responses to large-scale environmental change. In: J. G. Canadell, D. E. PatakiL. F. Pitelka eds. *Terrestrial Ecosystems in a Changing World*. Berlin, Germany: Springer, 175-192.

Rogers A. 2014. The use and misuse of $V_{c,max}$ in Earth System Models. *Photosynthesis Research* **119**(1-2): 15-29.

Sage R, Sharkey T, Pearcy R. 1990. The effect of leaf nitrogen and temperature on the CO_2 response of photosynthesis in the C_3 dicot *Chenopodium album* L. *Australian Journal of Plant Physiology* **17**(2): 135-148.

Sage RF, Kubien DS. 2007. The temperature response of C_3 and C_4 photosynthesis. *Plant Cell and Environment* **30**(9): 1086-1106.

Sage RF, Sharkey TD. 1987. The effect of temperature on the occurrence of O_2 and CO_2 insensitive photosynthesis in field-grown plants. *Plant Physiology* **84**(3): 658-664.

Sage RF, Sharkey TD, Seemann JR. 1988. The in-vivo response of the ribulose-1,5-bisphosphate carboxylase activation state and the pool sizes of photosynthetic metabolites to elevated CO_2 in *Phaseolus vulgaris* L. *Planta* **174**(3): 407-416.

Sage RF, Way DA, Kubien DS. 2008. Rubisco, Rubisco activase, and global climate change. *Journal of Experimental Botany* **59**(7): 1581-1595.

Salvucci ME, Crafts-Brandner SJ. 2004. Inhibition of photosynthesis by heat stress: the activation state of Rubisco as a limiting factor in photosynthesis. *Physiologia Plantarum* **120**(2): 179-186.

Scafaro AP, Von Caemmerer S, Evans JR, Atwell BJ. 2011. Temperature response of mesophyll conductance in cultivated and wild *Oryza* species with contrasting mesophyll cell wall thickness. *Plant, Cell & Environment* **34**(11): 1999-2008.

Schrader SM, Wise RR, Wacholtz WF, Ort DR, Sharkey TD. 2004. Thylakoid membrane responses to moderately high leaf temperature in Pima cotton. *Plant, Cell & Environment* **27**(6): 725-735.

Sellers PJ, Dickinson RE, Randall DA, Betts AK, Hall FG, Berry JA, Collatz GJ, Denning AS, Mooney HA, Nobre CA, Sato N, Field CB, Henderson-Sellers A. 1997. Modeling the exchanges of energy, water, and carbon between continents and the atmosphere. *Science* **275**(5299): 502-509.

Sharkey TD. 1985. O_2-insensitive photosynthesis in C_3 plants - Its occurrence and a possible explanation. *Plant Physiology* **78**(1): 71-75.

Sharkey TD, Bernacchi CJ, Farquhar GD, Singsaas EL. 2007. Fitting photosynthetic carbon dioxide response curves for C_3 leaves. *Plant, Cell & Environment* **30**(9): 1035-1040.

Sharkey TD, Berry JA, Sage RF. 1988. Regulation of photosynthetic electron-transport in *Phaseolus vulgaris* L., as determined by room-temperature chlorophyll a fluorescence. *Planta* **176**(3): 415-424.

Stitt M. 1991. Rising CO_2 levels and their potential significance for carbon flow in photosynthetic cells. *Plant, Cell & Environment* **14**(8): 741-762.

von Caemmerer S. 2000. *Biochemical models of leaf photosynthesis*. Collingwood, Australia: CSIRO Publishing.

von Caemmerer S, Evans JR. 2014. Temperature responses of mesophyll conductance differ greatly between species. *Plant Cell and Environment*: n/a-n/a.

von Caemmerer S, Evans JR. 2015. Temperature responses of mesophyll conductance differ greatly between species. *Plant, Cell & Environment* **38**(4): 629-637.

von Caemmerer S, Evans JR, Hudson GS, Andrews TJ. 1994. The kinetics of ribulose-1,5-bisphosphate carboxylase/oxygenase in vivo inferred from measurements of photosynthesis in leaves of transgenic tobacco. *Planta* **195**(1): 88-97.

von Caemmerer S, Farquhar GD. 1981. Some relationships between the biochemistry of photosynthesis and the gas exchange of leaves. *Planta* **153**(4): 376-387.

von Caemmerer S, Quick WP 2000. Rubisco: physiology in vivo. In: R. C. Leegood, T. D. SharkeyS. von Caemmerer eds. *Advances in Photosynthesis - Photosynthesis: Physiology and Metabolism*. Dordrecht, The Netherlands: Kluwer Academic Publishers, 83-113.

Walker B, Ariza LS, Kaines S, Badger MR, Cousins AB. 2013. Temperature response of *in vivo* Rubisco kinetics and mesophyll conductance in *Arabidopsis thaliana*: comparisons to *Nicotiana tabacum*. *Plant, Cell & Environment* **36**(12): 2108-2119.

Wise RR, Olson AJ, Schrader SM, Sharkey TD. 2004. Electron transport is the functional limitation of photosynthesis in field-grown Pima cotton plants at high temperature. *Plant, Cell & Environment* **27**(6): 717-724.

Yamori W, Irving LJ, Adachi S, Busch FA 2016. Strategies for optimizing photosynthesis with biotechnology to improve crop yield. In: M. Pessarakli ed. *Handbook of Photosynthesis, 3rd Edition*: CRC Press, Taylor & Francis Publishing Company, Florida, USA, 741-759.

Yamori W, Noguchi K, Hikosaka K, Terashima I. 2010. Phenotypic plasticity in photosynthetic temperature acclimation among crop species with different cold tolerances. *Plant Physiology* **152**(1): 388-399.

Yamori W, Noguchi KO, Terashima I. 2005. Temperature acclimation of photosynthesis in spinach leaves: analyses of photosynthetic components and temperature dependencies of photosynthetic partial reactions. *Plant, Cell & Environment* **28**(4): 536-547.

Yin XY, Struik PC, Romero P, Harbinson J, Evers JB, Van Der Putten PEL, Vos J. 2009. Using combined measurements of gas exchange and chlorophyll fluorescence to estimate parameters of a biochemical C_3 photosynthesis model: a critical appraisal and a new integrated approach applied to leaves in a wheat (*Triticum aestivum*) canopy. *Plant, Cell & Environment* **32**(5): 448-464.

The following Supporting Information is available for this article:

Fig. S1 Schematic representation of some of the processes that affect the rate of CO_2 uptake.

Fig. S2 Sample A/C_c and ETR/C_c responses

Fig. S3 Impact of the chosen value of α on *OS* and *CS*.

Fig. S4 Temperature response of modeled and measured sensitivities of *A* and *ETR* to a change in O_2 or CO_2 concentration at a light intensity of 250 µmol m^{-2} s^{-1}.

Fig. S5 The impact of the assumed g_m value on estimating biochemical limitations from O_2 or CO_2 sensitivities.

Notes S1 Derivations of the O_2 and CO_2 sensitivities of *ETR*

Notes S2 Estimation of CO_2 ranges for which intermediate values can be expected

867 # Tables

868

869 **Table 1**

870 List of acronyms, definitions and variables

Acronym/Variable	Definition	Unit
1-qP	PSII excitation pressure	
A	Net CO_2 assimilation rate	µmol m^{-2} s^{-1}
A_c	Rubisco limited CO_2 assimilation rate	µmol m^{-2} s^{-1}
A_j	RuBP regeneration limited CO_2 assimilation rate	µmol m^{-2} s^{-1}
A_p	Triose phosphate utilization limited CO_2 assimilation rate	µmol m^{-2} s^{-1}
C_a	CO_2 concentration outside the leaf	µmol mol^{-1}
C_c	CO_2 concentration in the chloroplast	µmol mol^{-1}
C_i	CO_2 concentration in the intercellular air space	µmol mol^{-1}
CS	CO_2 sensitivity	
CS(*A*)	CO_2 sensitivity of *A*	
CS(*ETR*)	CO_2 sensitivity of *ETR*	
ETR	Rate of photosynthetic electron transport (estimated by fluorescence)	µmol m^{-2} s^{-1}
ETR_c	Rubisco limited electron transport rate	µmol m^{-2} s^{-1}
ETR_j	RuBP regeneration limited electron transport rate	µmol m^{-2} s^{-1}
ETR_p	Triose phosphate utilization limited electron transport rate	µmol m^{-2} s^{-1}
g_m	Mesophyll conductance	mol m^{-2} s^{-1}
J	Rate of photosynthetic electron transport (estimated by gas exchange)	µmol m^{-2} s^{-1}
J_{max}	Maximum rate of photosynthetic electron transport	µmol m^{-2} s^{-1}
K_c	Michaelis-Menten constant of Rubisco for CO_2	µmol mol^{-1}
K_m	Michaelis-Menten constant of Rubisco for CO_2 in the presence of O_2	µmol mol^{-1}
K_o	Michaelis-Menten constant of Rubisco for O_2	mmol mol^{-1}
NPQ	Non-photochemical quenching	
O	Oxygen concentration	mmol mol^{-1}
OS	O_2 sensitivity	
OS(*A*)	O_2 sensitivity of *A*	
OS(*ETR*)	O_2 sensitivity of *ETR*	
R_d	Mitochondrial respiration	µmol m^{-2} s^{-1}
RuBP	Ribulose 1,5-bisphosphate	
T_p	Maximum rate of triose phosphate utilization	µmol m^{-2} s^{-1}
TPU	Triose phosphate utilization	
V_c	Rate of RuBP carboxylation	µmol m^{-2} s^{-1}
V_{cmax}	Maximum rate of Rubisco carboxylation	µmol m^{-2} s^{-1}
V_o	Rate of RuBP oxygenation	µmol m^{-2} s^{-1}
α	Fraction of photorespiratory carbon used for amino acid synthesis	
Γ*	CO_2 compensation point in the absence of mitochondrial respiration	µmol mol^{-1}

871

Figures

Figure 1

Variability of temperature responses of some commonly used parameters of the FvCB model. (a) CO_2 compensation point in the absence of mitochondrial respiration (Γ^*); (b) Michaelis Menten constant of Rubisco for CO_2 in the presence of O_2 ($K_m = K_c(1+O/K_o)$). The temperature responses of both Γ^* and K_m are derived from either *in vitro* (Badger & Collatz, 1977; Jordan & Ogren, 1984) or *in vivo* (Brooks & Farquhar, 1985; von Caemmerer, 2000; Bernacchi *et al.*, 2001; Bernacchi *et al.*, 2002; Walker *et al.*, 2013) measurements of Rubisco kinetics. (c) V_{cmax}; and (d) J_{max} of a selection of herbaceous plants. Hereby, some authors describe the temperature response with an Arrhenius-type equation, while others use a peaked function.

Figure 2

CO_2 response of modeled and measured sensitivities of the gross CO_2 assimilation rate and *ETR* to a change in O_2 or CO_2 concentration at 25°C. (a) O_2 sensitivity of *A*; (b) O_2 sensitivity of *ETR*; (c) CO_2 sensitivity of *A*; (d) CO_2 sensitivity of *ETR*. The O_2 sensitivity was estimated by a change in O_2 concentration from 21 to 2%. The CO_2 sensitivity was estimated by a change in CO_2 concentration of 30 µmol mol^{-1}. Lines show modeled sensitivities for A_c (red), A_j (green) and A_p (yellow) as the averages of seven published and commonly used sets of Rubisco kinetic parameters and the colored shaded areas denoting the range between the minimum and maximum of all values obtained. Hatched areas indicate the CO_2 ranges of where measured sensitivities will show values intermediate of two limitations due to limitation shifts when varying the O_2 or CO_2 concentration (see Supporting Information, Notes S2, for further details). Closed circles: measured sensitivities; n = 5 ± SE. The inserts in (c) and (d) show the same data of the main figure drawn to a different scale for clarity.

Figure 3

The CO_2 response of the photosynthetic electron transport rate (*ETR*) measured by chlorophyll fluorescence at six different measurement temperatures (15°, 20°, 25°, 30°, 35° and 40°C), as percentage of the maximum *ETR*. Black lines denote the averages and shaded areas the SE of 3 to 5 measurements. The lines and areas shaded in green show the range of chloroplastic CO_2 concentration (C_c) for which *ETR* is within 5% of the maximum *ETR*. Solid squares denote the averages of the measured values from which the CO_2 responses were derived.

Figure 4

The CO_2 response of the excitation pressure of PSII (1-qP) at six different measurement temperatures (15°, 20°, 25°, 30°, 35° and 40°C). Black lines denote the averages and shaded areas the SE of 3 to 5 measurements. The lines and areas shaded in green show the range of chloroplastic CO_2 concentration (C_c) for which 1-qP is within 0.01 of the minimum value of 1-qP. Solid squares denote the averages of the measured values from which the CO_2 responses were derived.

Figure 5

CO_2 response of the CO_2 assimilation rate (A) at six different measurement temperatures (15°, 20°, 25°, 30°, 35° and 40°C). Solid lines show A/C_c curves at 21% O_2, dashed lines at 2% O_2. The colored bars indicate the range of limitations estimated by the sensitivity of A and *ETR* to O_2 and CO_2. Red: A_c limited range; green: A_j limited range; yellow: A_p limited range. n = 3 to 5 ± SE. Symbols denote the average of the measured values from which the CO_2 responses were derived (solid squares: 21% O_2; open circles: 2% O_2).

Figure 6

Temperature responses of $A_{net}+R_d$ (a), *ETR* (b), and *NPQ* (c), measured at a light intensity of 250 µmol m^{-2} s^{-1} and two different CO_2 concentrations [380 (blue circles) and 1500 (red squares) µmol mol^{-1} CO_2] and O_2 [21% (solid symbols) and 2% (open symbols) O_2].

For clarity the temperature response of *NPQ* at 1500 / 2% is not shown, as it closely follows the response of *NPQ* at 1500 / 21%. n = 3 to 5 ± SE. Arrows indicate the temperature, at which *ETR* starts to decrease (b) and *NPQ* starts to increase with increasing temperature (c).

Figure 7

Temperature responses of A_{net}+R_d (a), *ETR* (b), and 1-qP (c), measured at a light intensity of 900 µmol m^{-2} s^{-1} and two different CO_2 concentrations [380 (blue circles) and 1500 (red squares) µmol mol^{-1} CO_2] and O_2 [21% (solid symbols) and 2% (open symbols) O_2]. n = 3 to 5 ± SE.

Figure 8

Temperature response of modeled and measured sensitivities of the gross CO_2 assimilation rate and *ETR* to a change in O_2 or CO_2 concentration at a light intensity of 900 µmol m^{-2} s^{-1}. O_2 sensitivities of *A* (a) and *ETR* (b) at a CO_2 concentration of 380 µmol mol^{-1}, estimated by a change in O_2 concentration from 21 to 2%. CO_2 sensitivities of *A* at 21% O_2 (c) and 2% O_2 (d), estimated by a change in CO_2 concentration from 380 to 1500 µmol mol^{-1}. Lines show modeled sensitivities for A_c (red), A_j (green) and A_p (yellow) as the averages of seven published and commonly used sets of Rubisco kinetic parameters at the C_c corresponding to the measured values of C_c for each temperature. The colored shaded areas denote the range between the minimum and maximum of all values obtained. Closed circles show the measured sensitivities estimated from the temperature responses shown in Figure 7a and b.

Figure 9

Measured rates of CO_2 assimilation (*A*) in response to chloroplastic CO_2 concentration (C_c) and leaf temperature. The color overlay indicates the process limiting *A* at any given condition, as determined by our sensitivity analysis derived from CO_2 response curves at six different leaf temperatures. Red: *A* is limited by Rubisco (A_c); green: *A* is limited by

959 RuBP regeneration (A_j); yellow: A is limited by TPU (A_p). The black line denotes A at the
960 C_c observed at an ambient C_a of 400 μmol mol^{-1} for the measurements reported here.

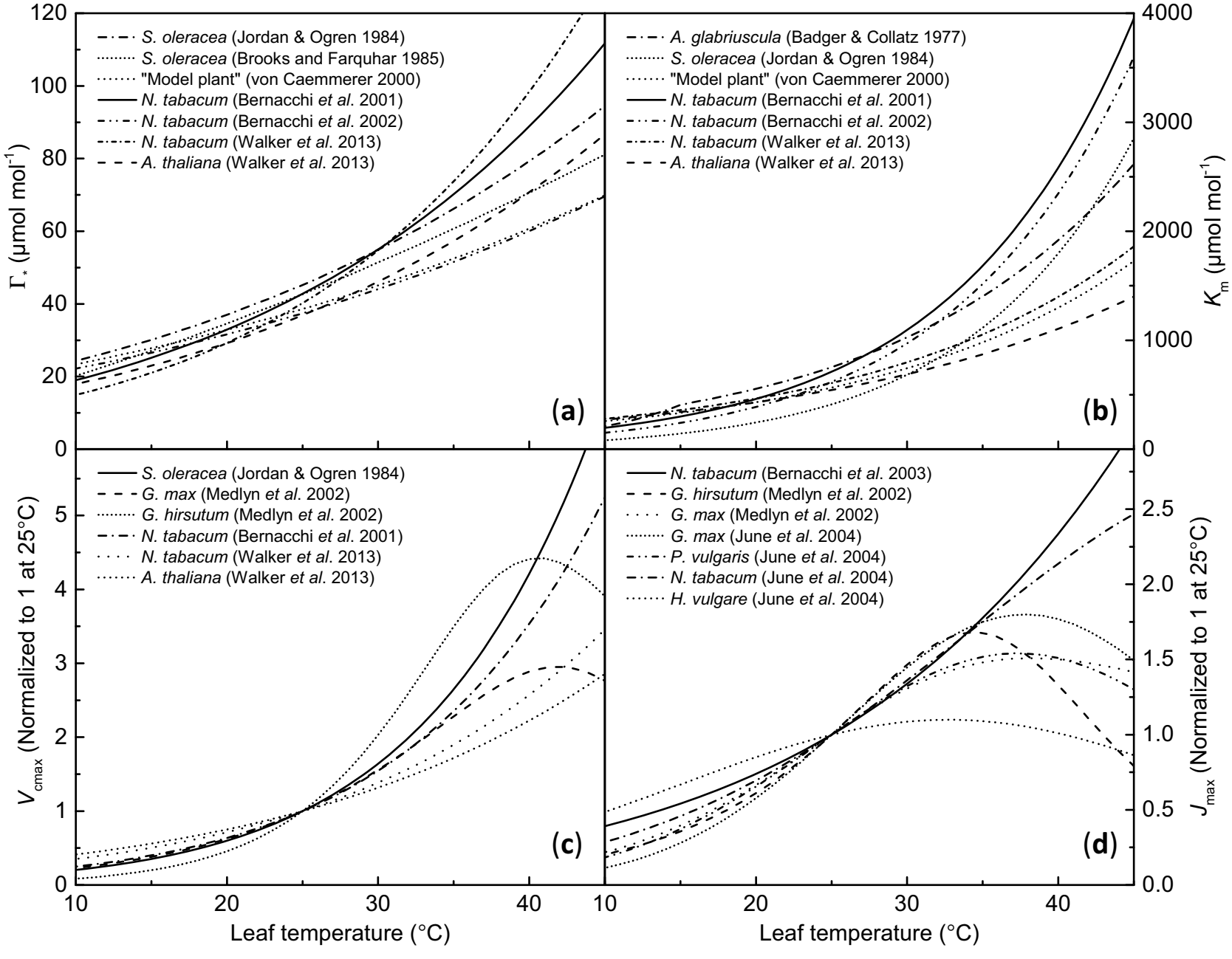
S. oleracea (Jordan & Ogren 1984)
S. oleracea (Brooks and Farquhar 1985)
"Model plant" (von Caemmerer 2000)
N. tabacum (Bernacchi et al. 2001)
N. tabacum (Bernacchi et al. 2002)
N. tabacum (Walker et al. 2013)
A. thaliana (Walker et al. 2013)
Γ* (μmol mol-1)
(a)
A. glabriuscula (Badger & Collatz 1977)
S. oleracea (Jordan & Ogren 1984)
"Model plant" (von Caemmerer 2000)
N. tabacum (Bernacchi et al. 2001)
N. tabacum (Bernacchi et al. 2002)
N. tabacum (Walker et al. 2013)
A. thaliana (Walker et al. 2013)
Km (μmol mol-1)
(b)
S. oleracea (Jordan & Ogren 1984)
G. max (Medlyn et al. 2002)
G. hirsutum (Medlyn et al. 2002)
N. tabacum (Bernacchi et al. 2001)
N. tabacum (Walker et al. 2013)
A. thaliana (Walker et al. 2013)
Vcmax (Normalized to 1 at 25°C)
(c)
N. tabacum (Bernacchi et al. 2003)
G. hirsutum (Medlyn et al. 2002)
G. max (Medlyn et al. 2002)
G. max (June et al. 2004)
P. vulgaris (June et al. 2004)
N. tabacum (June et al. 2004)
H. vulgare (June et al. 2004)
Jmax (Normalized to 1 at 25°C)
(d)
Leaf temperature (°C)
Leaf temperature (°C)

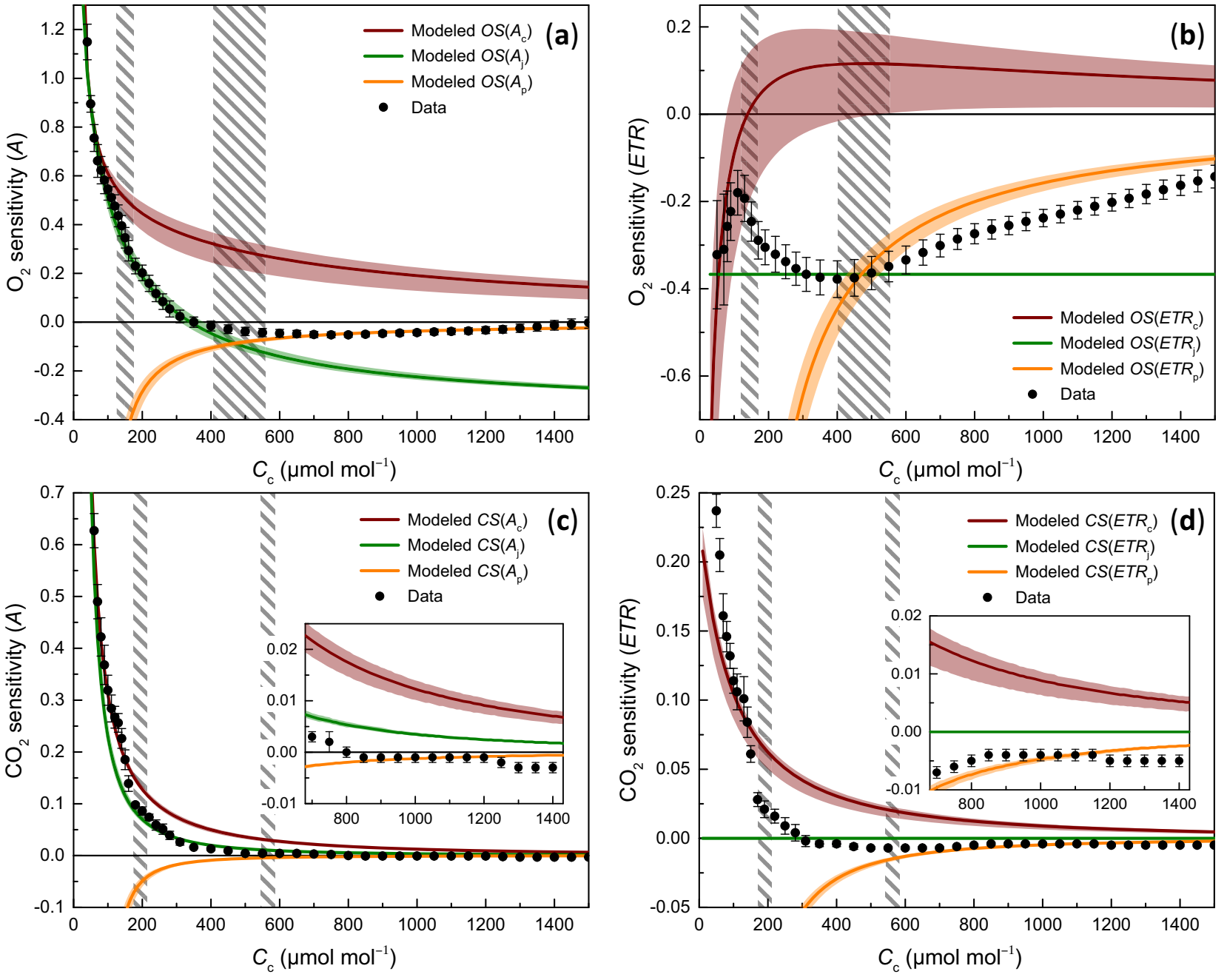
(a)
Modeled OS(A_c)
Modeled OS(A_j)
Modeled OS(A_p)
Data
O2 sensitivity (A)
C_c (μmol mol^-1)
(b)
Modeled OS(ETR_c)
Modeled OS(ETR_j)
Modeled OS(ETR_p)
Data
O2 sensitivity (ETR)
C_c (μmol mol^-1)
(c)
Modeled CS(A_c)
Modeled CS(A_j)
Modeled CS(A_p)
Data
CO2 sensitivity (A)
C_c (μmol mol^-1)
(d)
Modeled CS(ETR_c)
Modeled CS(ETR_j)
Modeled CS(ETR_p)
Data
CO2 sensitivity (ETR)
C_c (μmol mol^-1)

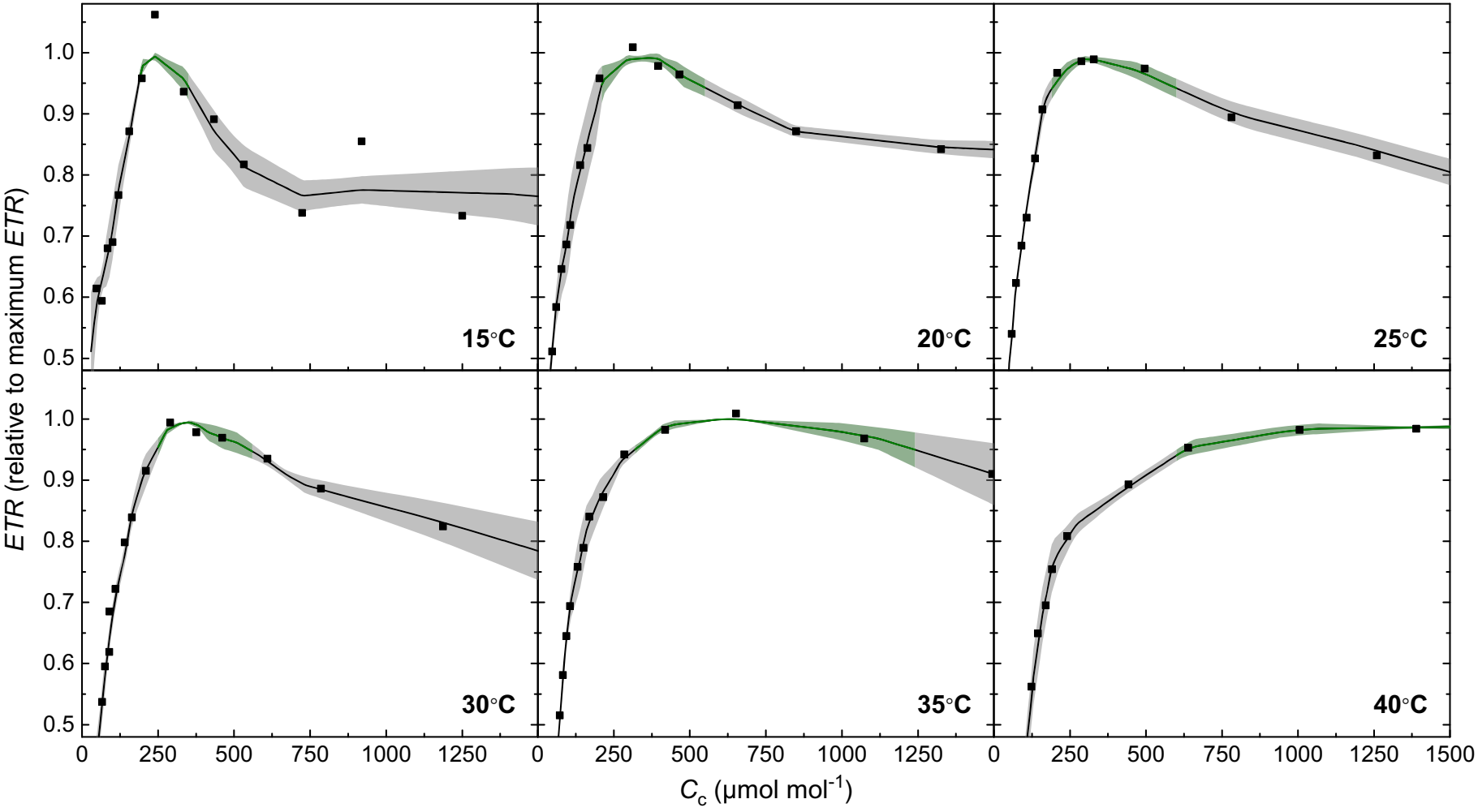
ETR (relative to maximum ETR)
1.0
0.9
0.8
0.7
0.6
0.5
15°C
20°C
25°C
30°C
35°C
40°C
0
250
500
750
1000
1250
1500
Cc (µmol mol-1)

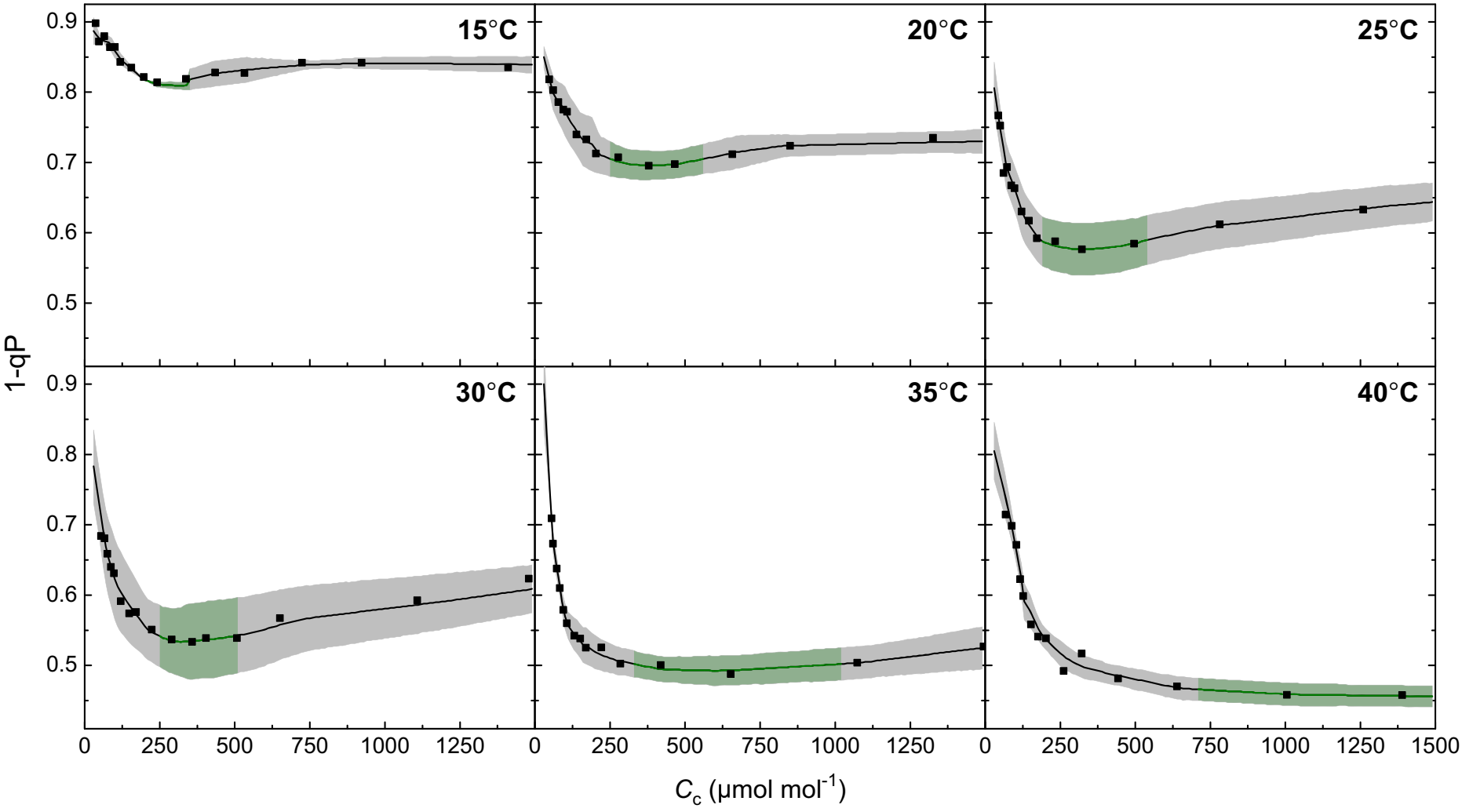
15°C
20°C
25°C
30°C
35°C
40°C
1-qP
0.9
0.8
0.7
0.6
0.5
0
250
500
750
1000
1250
1500
C_c (µmol mol^{-1})

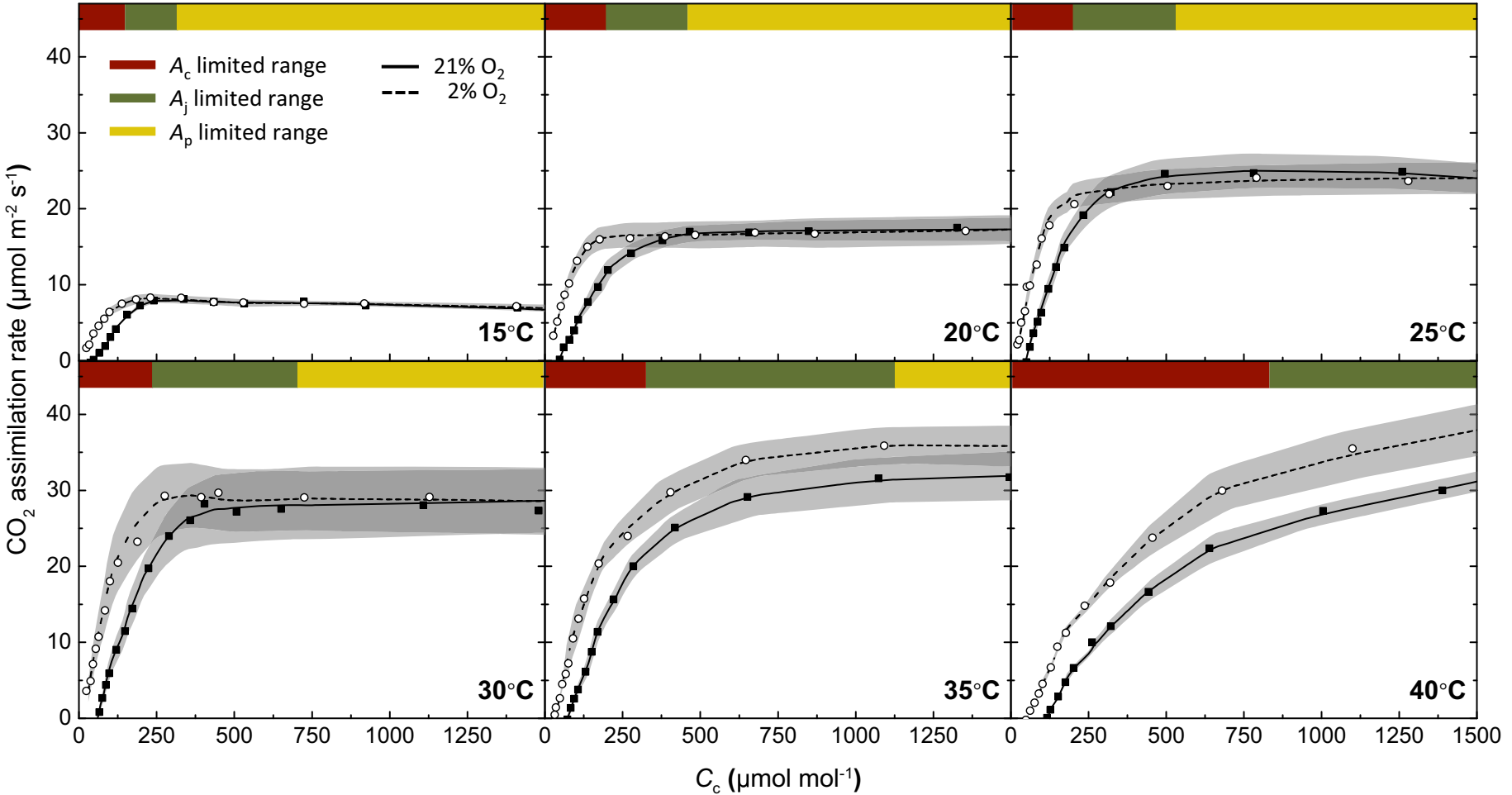
A_c limited range
A_j limited range
A_p limited range
21% O_2
2% O_2
15°C
20°C
25°C
30°C
35°C
40°C
CO_2 assimilation rate (µmol m^{-2} s^{-1})
C_c (µmol mol^{-1})
0
10
20
30
40
250
500
750
1000
1250
1500

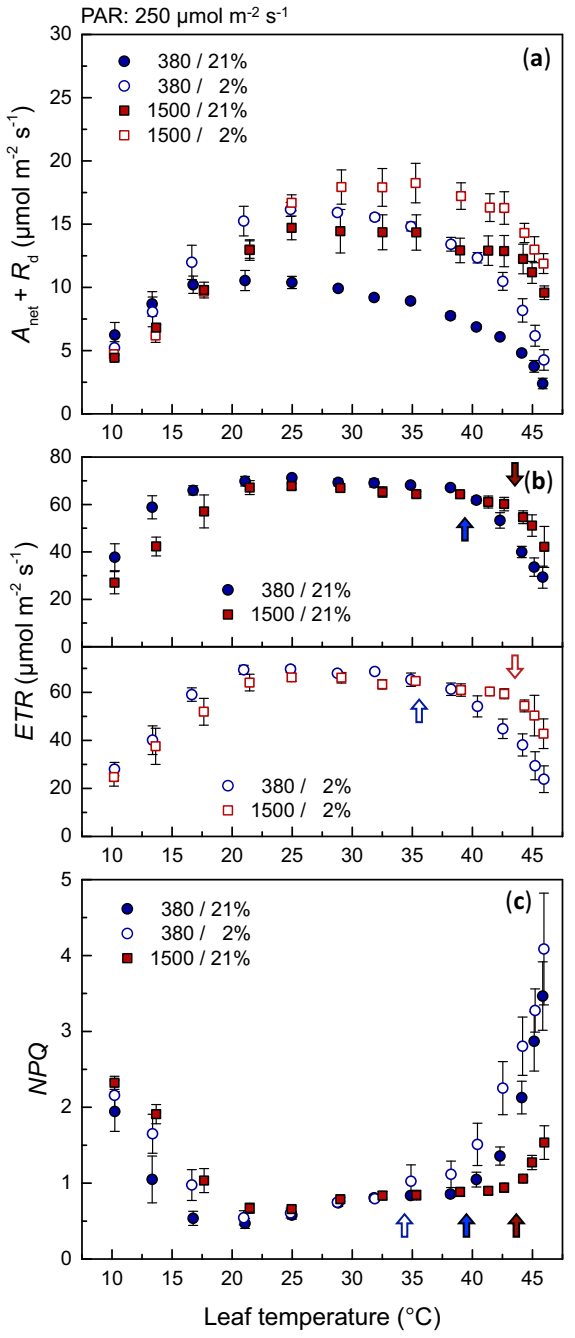
PAR: 250 µmol m-2 s-1
(a)
380 / 21%
380 / 2%
1500 / 21%
1500 / 2%
Anet + Rd (µmol m-2 s-1)
(b)
380 / 21%
1500 / 21%
380 / 2%
1500 / 2%
ETR (µmol m-2 s-1)
(c)
NPQ
Leaf temperature (°C)

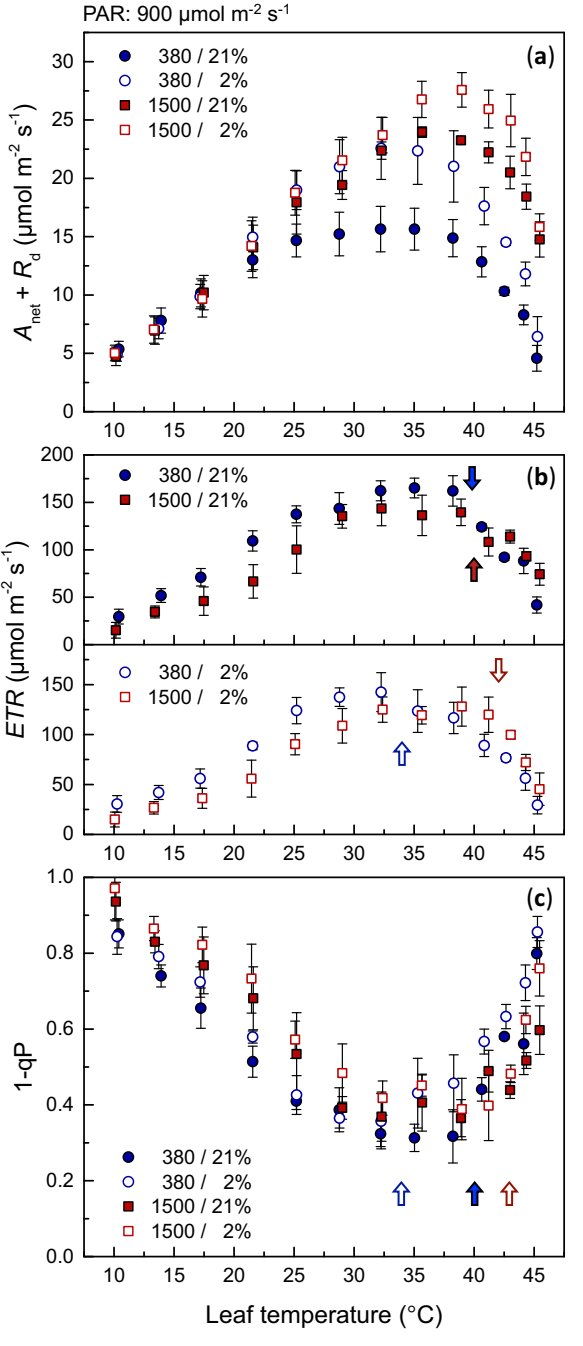
PAR: 900 µmol m-2 s-1
(a)
380 / 21%
380 / 2%
1500 / 21%
1500 / 2%
Anet + Rd (µmol m-2 s-1)
(b)
380 / 21%
1500 / 21%
380 / 2%
1500 / 2%
ETR (µmol m-2 s-1)
(c)
380 / 21%
380 / 2%
1500 / 21%
1500 / 2%
1-qP
Leaf temperature (°C)

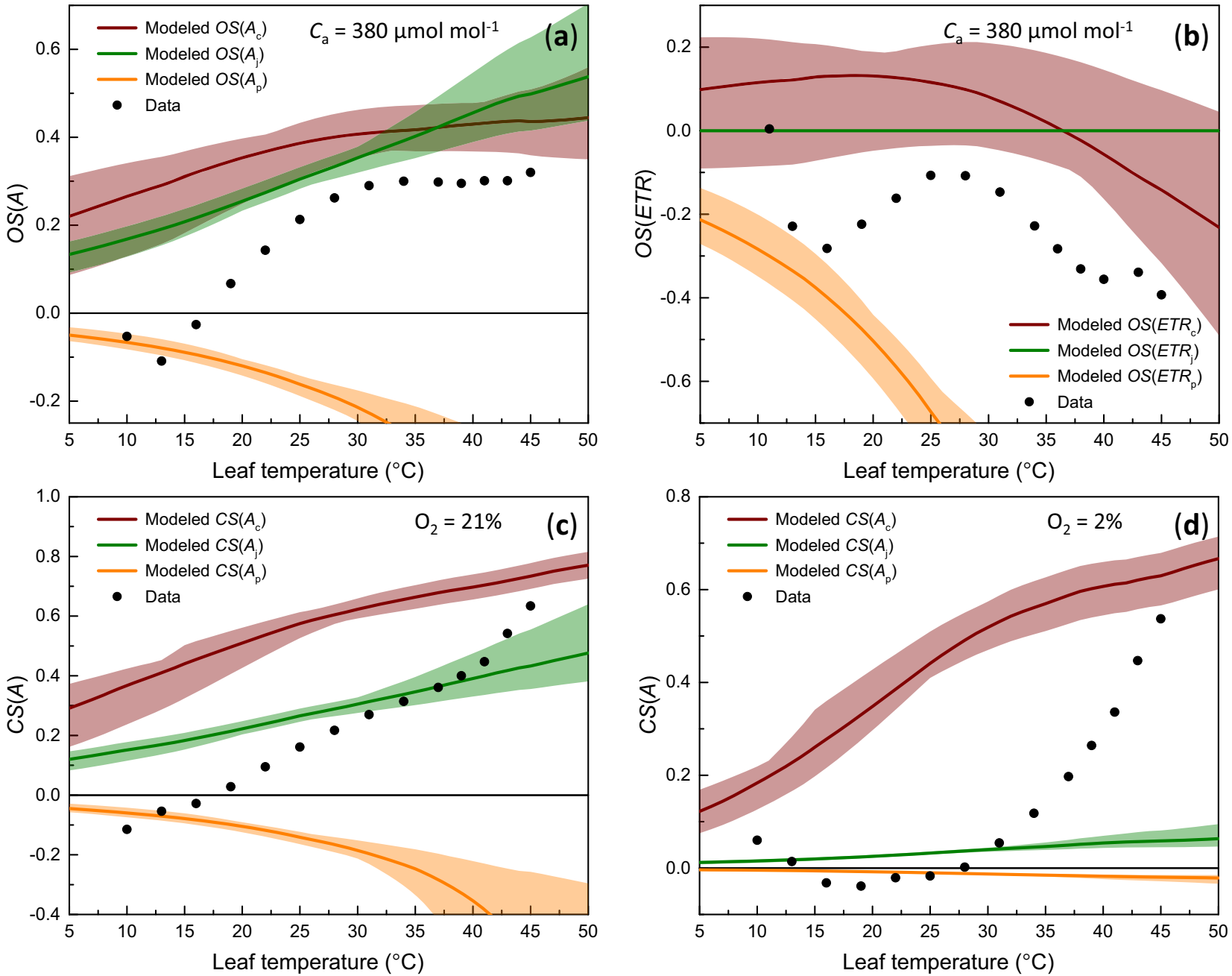
(a)
C_a = 380 µmol mol^{-1}
Modeled $OS(A_c)$
Modeled $OS(A_j)$
Modeled $OS(A_p)$
Data
$OS(A)$
Leaf temperature (°C)
(b)
C_a = 380 µmol mol^{-1}
Modeled $OS(ETR_c)$
Modeled $OS(ETR_j)$
Modeled $OS(ETR_p)$
Data
$OS(ETR)$
Leaf temperature (°C)
(c)
O_2 = 21%
Modeled $CS(A_c)$
Modeled $CS(A_j)$
Modeled $CS(A_p)$
Data
$CS(A)$
Leaf temperature (°C)
(d)
O_2 = 2%
Modeled $CS(A_c)$
Modeled $CS(A_j)$
Modeled $CS(A_p)$
Data
$CS(A)$
Leaf temperature (°C)

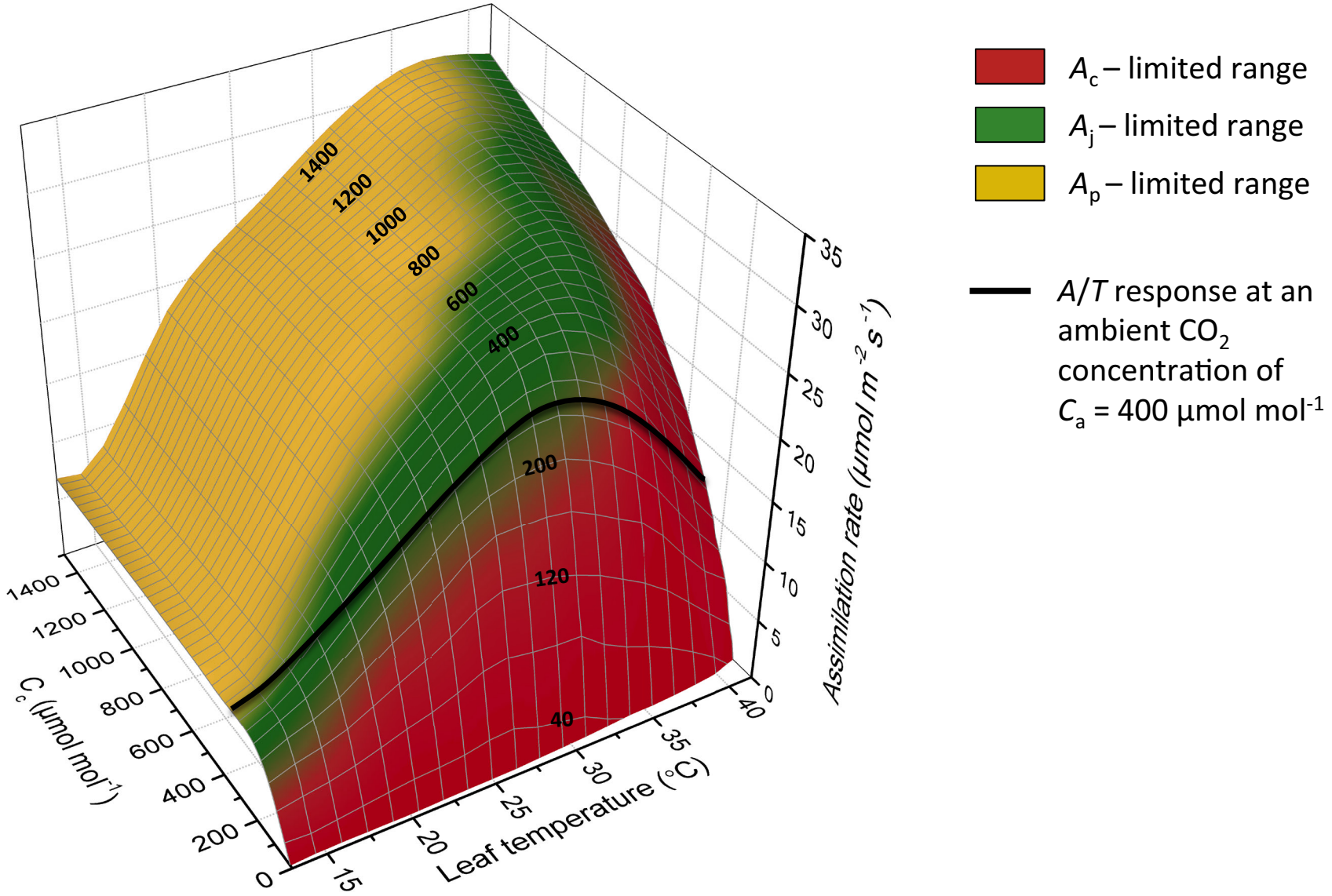
A_c – limited range
A_j – limited range
A_p – limited range
A/T response at an ambient CO_2 concentration of C_a = 400 µmol mol^{-1}
1400
1200
1000
800
600
400
200
120
40
C_c (µmol mol^{-1})
Leaf temperature (°C)
Assimilation rate (µmol m^{-2} s^{-1})